

# **“Design of Ultra-Wideband 3dB Tandem Hybrid Coupler using Multi-Element Coupled Lines”**

Dissertation submitted towards the partial fulfillment of requirement for the award of  
degree of

**Master of Engineering**

**In**

**Wireless Communications**

Submitted by:

**Abhinav Jain**

**Roll No: 801463001**

Under the guidance of:

**Dr. Rana Pratap Yadav**

**(Assistant Professor, ECED)**



**ELECTRONICS AND COMMUNICATION ENGINEERING  
DEPARTMENT**

**THAPAR UNIVERSITY**

**(Established under the section 3 of UGC Act, 1956)**

**PATIALA – 147004 (PUNJAB)**

**July 2016**

## CERTIFICATE

I hereby certify that the work which is being presented in the Dissertation entitled "Design of Ultra-Wideband 3dB Tandem Hybrid Coupler using Multi-Element coupled lines" is an authentic record of my study carried out as requirement for the award of degree of Master of Engineering in Wireless Communications at Thapar University, Patiala, under the supervision of **Dr. Rana Pratap Yadav, Assistant Professor, Electronics and Communication Department (ECED)**. The matter presented in the dissertation has not been submitted in any other University/Institute for the award of degree.

Date: 13 June 2016

  
**Abhinav Jain**

Roll No. 801463001

It is certified that the above statement made by the student is correct to the best of my knowledge and belief.

Date: 13/06/16

  
**Dr. Rana Pratap Yadav**

Assistant Professor, ECED

Thapar University, Patiala

Countersigned by

  
**Dr. Sanjay Sharma**

Professor and Head (ECED)

Thapar University, Patiala

  
**Dr. S. S. Bhatia**

Dean, Academic Affairs

Thapar University, Patiala

## **ABSTRACT**

Dissertation presents the design and simulation of 50W, 140-240MHz, 3dB hybrid coupler using multi-element coupled lines and its applicability in development of mock-up fast RF matching network is discussed. In mock-up RF matching network, 3dB hybrid coupler is used to divide the RF power coming from the RF source and it also provides essential protection to the RF generator by coupling of reflected power to isolated port. A single quarter wavelength coupled element provides narrow frequency band and is used in development of narrow band 3dB hybrid coupler. For the broadband applications, multi-element coupled lines are used where several number of quarter wavelength element are cascaded in a specific manner. Coupling of each of the cascaded element is calculated using theory of equal ripple polynomial i.e. based on curve fitting method. This theory is also explained in detail in thesis and values of coupling for 3-elements coupled lines are derived. In multi-element coupled lines, coupling of middle element is found to be much higher as compared to side elements and provide small gap between the coupled lines. The increase in number of elements provide very narrow coupling gap and at a certain limit its fabrication becomes very difficult. Therefore, development of broadband 3dB coupler using single section of multi-element coupled lines could not be possible due to fabrication constraints. To achieve the wider coupling gap in middle element, two broad band 8.34dB multi-elements sections are connected in tandem to have overall 3dB coupling. Initially a narrow band single element 3dB hybrid coupler is designed, simulated and presented in detail. It provides very narrow frequency band which is not sufficient for the application of mock-up RF system and therefore, ultra-wide band hybrid coupler is designed. Here, result of both the devices is presented in comparative manner.

## ACKNOWLEDGEMENT

First of all, I would like to express my gratitude to **Dr. RANA PRATAP YADAV, Assistant Professor**, Electronics and Communication Engineering Department, Thapar University, Patiala for his patient guidance and support throughout this report. I am truly very fortunate to have the opportunity to work with him. I found his guidance to be extremely valuable.

I am also thankful to our **Head of the Department, Dr. Sanjay Sharma** as well as **P.G. coordinator Dr. Amit Kumar Kohli, Associate Professor, ECED, Thapar University, Patiala**. The completion of any project is the endeavor of all individuals that supports, include & foster the much needed enthusiasm and confidence to the doer of the project work within the whole task prove to be impossible mission.

I am pleased to write these lines for over whelming support of staff members of ECED, Thapar University for their invaluable contribution during my work. Their suggestions added more charm and information in preparing this report.

My greatest thanks to all who wished me success especially my friends for their years of unyielding love and support. I admire their determination, encouragement and support I thank the almighty--the supreme and the only supernatural power for imparting me courage, confidence to attain a full stop for this project.

Finally, I would like to thanks my parents for their years of unyielding love and support.

Date: \_\_\_\_\_

Place: Patiala

Abhinav Jain

M.E. (801463001)

# CONTENTS

<i>CERTIFICATE</i>	i
<i>ABSTRACT</i>	ii
<i>ACKNOWLEDGEMENT</i>	iii
<i>CONTENTS</i>	iv
<i>LIST OF ABBREVIATIONS</i>	vi
<i>LIST OF FIGURES</i>	vii
<i>LIST OF TABLES</i>	ix
<b>1. Introduction</b>	<b>1</b>
1.1. Preamble	1
1.2. Single Element coupled line	1
1.2.1. General Properties of Coupler	2
1.2.2. Coupling factor	4
1.2.3. Insertion Loss	4
1.2.4. Isolation Loss	4
1.2.5. Directivity	5
1.3. Mode Analysis	5
1.3.1. Odd Mode Analysis	6
1.3.2. Even Mode Analysis	7
1.4. Multi-section coupled lines coupler	7
1.4.1. Analysis of single section coupler	8
1.4.2. Derivation of Coupler Parameter	9
<b>2. Literature Survey</b>	<b>15</b>
<b>3. Choice of Transmission Line</b>	<b>20</b>
3.1. Introduction	20
	iv

3.2. Review of Transmission Line Theory	20
3.2.1. Choice of Transmission Lines	23
3.2.2. Strip Line	23
<b>4. Comparison between Single Element and Multi-element Coupled Lines</b>	<b>29</b>
4.1. Introduction	29
4.2. For Single Coupled line section	30
4.3. For Multi-element Coupled line section	31
4.3.1. Three-Element Coupled line section	32
4.3.2. Five-Element Coupled line section	33
4.3.3. Seven-Element Coupled line section	34
<b>5. Design of 3dB Tandem Hybrid Coupler with Single Element</b>	<b>35</b>
5.1. Introduction	35
5.2. Concept and Design of 3dB Tandem Hybrid Coupler	36
5.2.1. Coupled Strip-line design	37
5.2.2. Non-Coupled Strip-line design	38
5.3. Calculated S-Parameters for Single–element 3dB Tandem Hybrid Coupler	40
<b>6. Design of 3dB Tandem Hybrid Coupler with Multi-Elements</b>	<b>44</b>
6.1. Introduction	44
6.2. Simulation using HFSS of 3dB Tandem three element coupler	47
6.3. Calculated S-Parameters for Three–element 3dB Tandem Hybrid Coupler	51
<b>7. Concluding Remarks and Future Scope</b>	<b>55</b>
7.1. Conclusion	55
7.2. Future Scope	56
<b><u>References</u></b>	<b>57</b>

## **LIST OF ABBREVIATIONS**

RF	radio frequency
DC	Direct coupled
UHF	Ultra High Frequency
VHF	Very High Frequency
TEM	Transverse Electromagnetic
VSWR	Voltage Standing Wave Ratio
dB	Decibel
Fig	Figure
ICRH	Ion Cyclotron Resonance Heating

## LIST OF FIGURES

<b>S.NO.</b>	<b>FIGURE</b>	<b>PAGE NO.</b>
1.1	4-port $\lambda/4$ coupled line section	2
1.2	Cross-sectional view of four widely used TEM coupled line pair	3
1.3	Transmission line and Capacitive network	5
1.4	Coupler with Plane of Symmetry	6
1.5	Odd mode Analysis	6
1.6	Even mode Analysis	7
1.7	Multi-element coupler of length $\lambda/4$ and junction of length $l$	8
1.8	Prototype of 3-elements, 3.01 dB coupled line section	8
1.9	Characteristic of 3-elements, 8.34 dB section using table values of crystal	14
3.1(a)	Transmission line	20
3.1(b)	Transmission line lumped equivalent circuit	21
4.1	Characteristic of single-element, 8.34dB coupled line section	31
4.2	N-section multi-element coupler	31
4.3	Characteristic of 3-elements, 8.34dB coupled line section using Cristal theory	32
4.4	Characteristic of 5-elements, 8.34dB coupled line section using Cristal theory	33
4.5	Characteristic of 7-elements, 8.34dB coupled line section using Cristal theory	34
5.1	Tandem 3dB hybrid Coupler	36
5.2	Simplified diagram of Single 8.34dB Coupled strip-line	37
5.3	Dimensions of the coupled line section	38
5.4	Dimensions of the Non-coupled line section	39
5.5	Return Loss of 3dB tandem hybrid coupler	40
5.6	Output of 3dB tandem hybrid coupler	41
5.7	Coupling of 3dB tandem hybrid coupler	42

5.8	Isolation of 3dB tandem hybrid coupler	43
6.1	Symmetrical 8.34dB coupled section with three elements	45
6.2(a)	Dimensions of Element-A	45
6.2(b)	Dimensions of Element-B	46
6.3(a)	Simulated result of Coupling for element-A using HFSS	47
6.3(b)	Simulated result of Coupling for element-B using HFSS	48
6.4	Simulated result of 3-elements, 8.34dB coupled line section using HFSS	49
6.5	Dimensions of connecting line	49
6.6	Schematic 3dB tandem hybrid coupler of three elements	50
6.7	Return Loss of 3dB tandem hybrid coupler for three element	51
6.8	Output of 3dB tandem hybrid coupler for three element	52
6.9	Coupling of 3dB tandem hybrid coupler for three element	53
6.10	Isolation of 3dB tandem hybrid coupler for three elements	54

## LIST OF TABLES

<b>S.NO.</b>	<b>TABLE</b>	<b>PAGE NO.</b>
1.1	Characteristics impedance values for 3-element coupled line	14

### 1.1 Preamble

Coupler based on single element works in a narrow frequency band and thus, has confined applications. For the ultra-wide band applications, multi-element coupled lines are used where several number of quarter wavelength elements are cascaded in a specific manner. The ultra-wide band coupled lines can be used to achieve the wider bandwidth in RF components such as balanced amplifiers, balanced modulator, power measurements and antenna array networks. These components are utilized in the area of satellite communication, defense, broadcast, and aerospace. One of its most desired applications is the development of 3dB hybrid coupler based on strip-line in VHF range.

3dB hybrid coupler is used to divide the RF power coming from the RF source and it also provides essential protection to the RF generator by coupling of reflected power to isolated port.

### 1.2 Single Element Coupled Line Coupler

Two transmission lines in proximity are used to obtain coupled line coupler such that power is delivered from the one line to other. Usually, we mostly deal with the lines that are coupled over a single quarter wave section, or multiple sections.

In order to get a quadrature coupled-line coupler, a quarter-wave section needs to be coupled. This leaves two broad categories of coupled line couplers [1]:

1. Edge coupled
2. Broadside coupled

Both these can be realized in micro strip, strip line or even coax.

For a usable coupler, there are two things necessary for directivity and quadrature phase:

1. The coupled section should be a quarter-wave at center frequency.
2. The product of even and odd mode impedances must be equal to  $Z_0^2$ .

### 1.2.1 Properties of Coupler

The coupler, as given in Fig. 1.1, consists of two transmission lines 1-2 and 3-4 with uniform spacing having length  $\lambda/4$ .

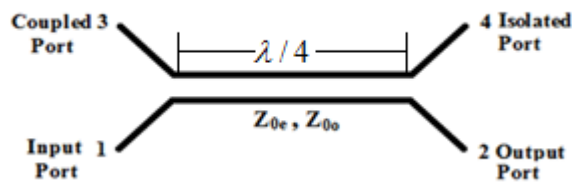


Fig. 1.1 4-port  $\lambda/4$  coupled line section

This coupler has an Input port, Output port, Coupled port and Isolated port as Port 1, Port 2, Port 3 and Port 4, respectively. Coupled transmission line coupler has the following properties when a signal generator is connected to Port 1, regardless of whether it is symmetrical or not [2]:

- Power transfer from port1 to 2
- Power transfer from port 1 to 3
- No power transfer from port 1 to 4
- No reflected wave out of port 1

A symmetrical directional coupler has symmetry with respect to the two planes. Port 1 and Port 2 have end-to-end symmetry with respect to Port 3 and Port 4; Port 2 and Port 3 have side to side symmetry with respect to Port 1 and Port 4.

One of the unique properties of a symmetrical coupler is that the two outputs at Port 2 and 3 have  $90^0$  phase difference between them at all frequencies.

In 1954, Oliver [1] and Firestone [3] showed that the natural electric and magnetic coupling between a pair of TEM transmission line produces directional coupling. Specifically, a wave is induced from one lineto another that propagates in the opposite direction. The TEM mode quarter-wave coupled transmission line coupler is shown in Fig1.1 above.

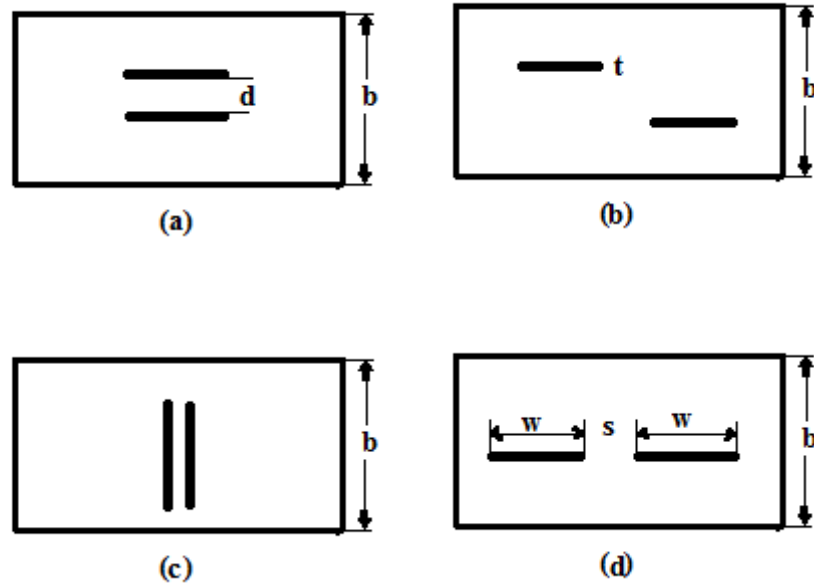


Fig. 1.2 Cross-sectional view of four widely used TEM coupled line pair.

Selection of structural configuration of the coupled lines is based on the coupling values. The configuration in part (a) and (c) are used if tight coupling (6dB or greater) is required where part (a) is often used in the design of 3dB couplers. For the loose coupling, coplanar strip line arrangement as shown in part (b) and (d) are most commonly used. The coupled lines shown in Fig. 1.2 consist of three conductors and represent the two transmission lines with common ground. Superposition of amplitudes of even and odd mode corresponds to excitation in the coupled lines [4]. In even mode, current in strip conductors has same amplitude and direction, whereas in odd mode, current in strip conductors has same amplitude but flow in opposite direction.

Coupling coefficient, i.e.  $C$ , of the coupled lines depends on the even and odd mode impedance values given by

$$C = \frac{Z_{0e} - Z_{0o}}{Z_{0e} + Z_{0o}}$$

here,  $Z_{0e}$  and  $Z_{0o}$  can be expressed as

$$Z_{0e} = Z_o \sqrt{\frac{1+C_v}{1-C_v}},$$

$$Z_{0o} = Z_o \sqrt{\frac{1 - C_v}{1 + C_v}}$$

For input power P1, output power P2, output power from the coupled port P3 and power output from the isolated port P4, some of the characteristics of the coupled line coupler are defined as:

### 1.2.2 Coupling factor

The coupling factor is given as:

$$C_{3,1} = 10 \log\left(\frac{P_1}{P_3}\right) dB$$

The coupling is defined as the power incident at input port to the power coupled at the coupled port. Coupling is a measure of how much of the incident power is being sampled.

### 1.2.3 Insertion loss

Insertion loss:

$$L_{2,1} = 10 \log\left(\frac{P_1}{P_2}\right) dB$$

Insertion loss is defined as the ratio of amount of power incident at input port to the amount of power received at the output port.

### 1.2.4 Isolation

Isolation is given as:

$$I_{4,1} = -10 \log\left(\frac{P_4}{P_1}\right) dB$$

Isolation is defined as the difference in signal level between the input port and the isolated port when the other two ports are terminated by the matched load.

### 1.2.5 Directivity

Directivity is given as:

$$D_{3,4} = -10\log\left(\frac{P_4}{P_3}\right) = -10\log\left(\frac{P_4}{P_1}\right) + 10\log\left(\frac{P_3}{P_1}\right)dB$$

Directivity is defined as ratio of power output in coupled arm to the power flowing in isolated port. Directivity is a measure of how well the coupler distinguishes between forward and reverse travelling waves.

### 1.3 Mode Analysis

It is found that the transmission lines are capacitive coupled such that it appears as if these lines are connected by capacitors.



Fig. 1.3 Transmission line and Capacitive network [4]

A plane of symmetry exists when the two transmission lines are same. As a result, this circuit can be analysed using odd and even mode analysis.

Under the identical condition of the two-transmission line,  $C_{11}=C_{22}$ .

Note in Fig. 1.4 below that the capacitor  $C_{12}$  has been divided into two capacitors connected in series, each with a value of  $2C_{12}$ .

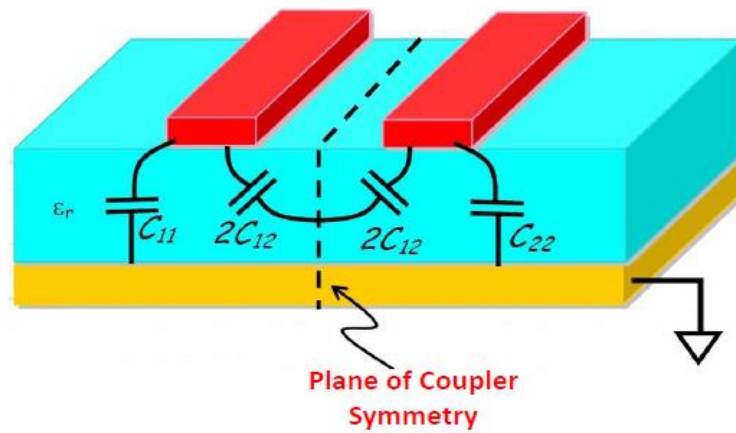


Fig. 1.4 Coupler with Plane of Symmetry [5]

### 1.3.1 Odd Mode Analysis

When incident wave in the two lines is opposite in the odd mode analysis such that they are equal in magnitude but  $180^\circ$  out of phase, a virtual ground plane is formed at plane of symmetry.

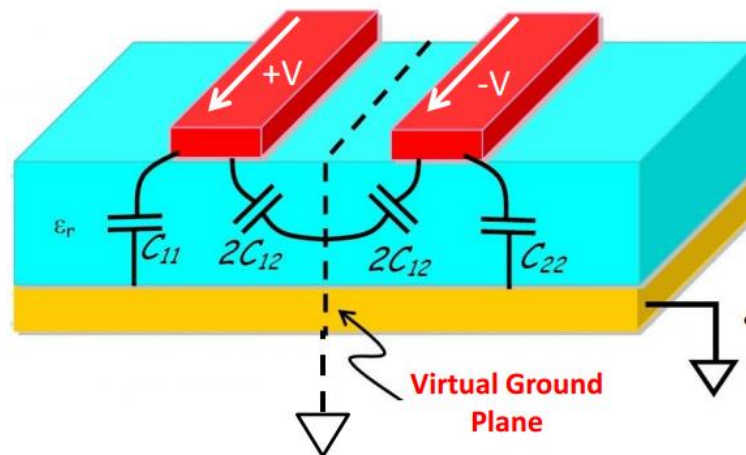


Fig. 1.5 Odd Mode Analysis [5]

In odd mode, capacitance per unit length is given by:

$$C_o = C_{11} + 2C_{12} = C_{22} + 2C_{12}$$

The corresponding characteristic impedance is:

$$Z_{0o} = \sqrt{\frac{L}{C_o}}$$

### 1.3.2 Even Mode Analysis

When incident wave in the two lines is equal in the even mode analysis such that they are equal in magnitude and phase, a virtual open plane is formed at plane of symmetry.

It is worth noting that the two  $2C_{12}$  capacitors are disconnected, and thus capacitance per unit length, in the even mode is given by:

$$C_e = C_{11} = C_{22}$$

Therefore the corresponding characteristic impedance is:

$$Z_{0e} = \sqrt{\frac{L}{C_e}}$$

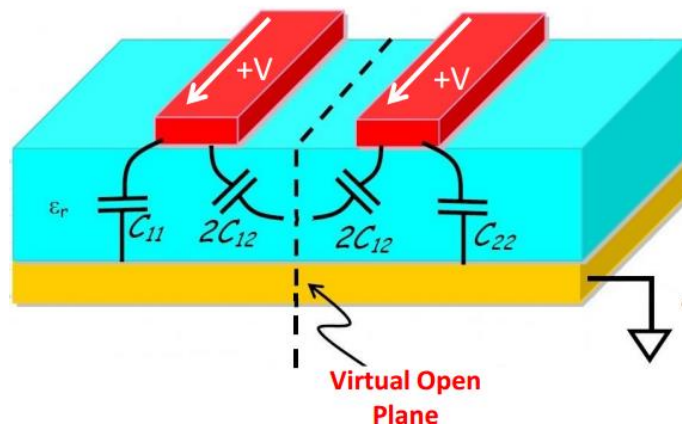


Fig. 1.6 Even Mode Analysis [5]

### 1.4 Multi-section Coupled-Line Couplers

Multiple coupled lines are added in series to increase coupler bandwidth. The couplers are typically designed such that they are symmetric, i.e., here, N is odd such that the phase characteristics are better. The design parameters for maximum coupling are same as 4-port coupler.

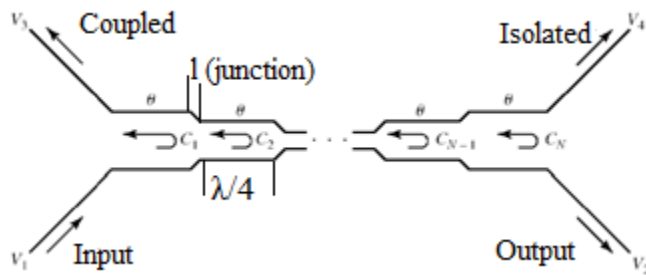


Fig. 1.7 Multi-element coupler of length  $\lambda/4$  and junction of length  $l$  [5]

The coupler based on single element works in narrow frequency band and thus has confined or limited applications. For the ultra-wide band applications, multi-element coupled lines are used where several number of quarter wavelength elements are cascaded in specific manner. Normally the odd numbers of elements are connected to form a coupled line coupler, this is because of the phase characteristics usually better when odd number are connected and each of the element of the coupler have  $\lambda/4$  length requirement. Stripline technology is preferable for the multi-element coupled line couplers. The Mismatched in the phase velocities will degrade the coupler properties, load mismatches, and fabrication tolerances.

### 1.4.1 Coupled Line Section with Three Elements

The diagram of 3-element symmetrical coupled line coupler is given in Fig. 1.8, where the element-B on both side of element-A are identical. Every element has the length of  $\lambda/4$  and also has four ports shown in diagram represented as input port, output port, coupled port, isolated port.

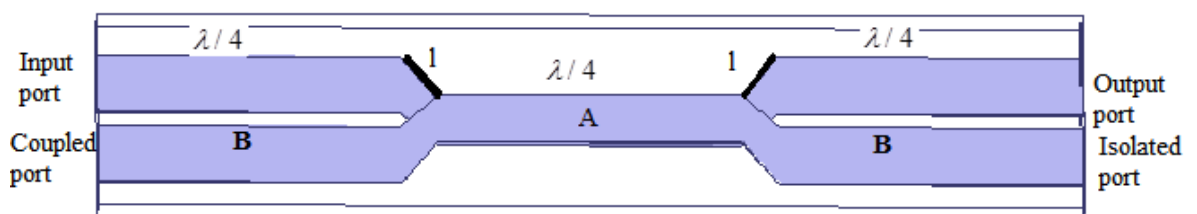


Fig. 1.8 Prototype of 3-elements, 3.01 dB coupled line coupler

$$\sqrt{Z_{0eA}Z_{0oA}} = \sqrt{Z_{0eB}Z_{0oB}}$$

where,  $Z_{0eA}$ ,  $Z_{0eB}$  are normalized even mode impedance of element-A and  $Z_{0oA}$ ,  $Z_{0oB}$  odd mode impedances of element-B.

### 1.4.2 Derivation of Coupler Parameter

From the Given Insertion-loss function, the derivation of the coupler parameter is presented here as:

- The necessary and sufficient condition for having an insertion loss function  $L$  represent a symmetrical network is of the form [2]:

$$L = 1 + [P_n(\sin\Theta)]^2$$

- The synthesis of a symmetrical directional coupler can be stepped as:
  1. Finding the optimum odd polynomial  $P_n(\sin\Theta)$
  2. Extracting the transmission-line impedances from the resulting insertion-loss function.

The derivation of the coupler parameters from the given insertion-loss function is presented as step by step procedure.

- Let  $P_n(x)$  be an odd polynomial in  $x$  of degree  $n$  that makes the function-

$$L(x) = 1 + P_n^2(x) \quad (1)$$

an equal ripple function on the interval 0 to 1.

Function  $L(x)$  may be identified as an equal-ripple insertion-loss function.

- From above equation, the magnitude square of the reflection coefficient is obtained as:

$$|\Gamma|^2 = \frac{P_n^2(x)}{1 + P_n^2(x)} \quad (2)$$

where,  $\Gamma$  is reflection coefficient.

- Richard's transformation is applied in two parts:
- Replace  $x$  by  $\frac{\hat{s}}{j}$

- Replace  $\frac{\hat{s}}{j}$  by  $\frac{\hat{(\frac{s}{j})}}{\sqrt{1+(\frac{\hat{s}}{j})^2}}$

Using the two part transformation process, the synthesis procedure is as follows:

❖ **Step A:**

Factoring is simplified by solving the lower order equations to find the roots:

1.  $p_n(s/j) = 0$

2.  $p_n(s/j) = \pm j$

❖ **Step B:**

Zeros of numerator and denominator mapped to new zeros

➤  $z'_i = \frac{z_i}{\sqrt{1+(z_i)^2}}$

➤  $p'_i = \frac{p_i}{\sqrt{1+(p_i)^2}}$

- The complex reflection coefficient given as:

$$\Gamma(s) = \frac{a \prod_{i=1}^n (s - z'_i)}{b \prod_{i=1}^n (s - p'_i)}$$

❖ **Step C:**

The constants a and b evaluated as

$$a = \left\{ \frac{(-1)^n p_n^2(\sqrt{2})}{\prod_{i=1}^n (s - z_i') \prod_{i=1}^n (-s - z_i')} \right\}_{s=\sqrt{2}}^{1/2} \quad b = \left\{ \frac{(-1)^n [1 + p_n^2(\sqrt{2})]}{\prod_{i=1}^n (s - p_i') \prod_{i=1}^n (-s - p_i')} \right\}_{s=\sqrt{2}}^{1/2}$$

$$p_n^2(\sqrt{2}) = a^2 \frac{\prod_{i=1}^n (s - z_i') \prod_{i=1}^n (-s - z_i')}{(-1)^n} \Bigg|_{s=\sqrt{2}}$$

❖ **Step D:**

Impedance function determined from reflection coefficient

$$Z(s) = \frac{1 + \Gamma'}{1 - \Gamma'} = \frac{Y_d' + Y_n'}{Y_d' - Y_n'}$$

- From Z the ABCD transmission matrix is constructed
- ❖ A is identified with the even part of  $Y_d' + Y_n'$
- ❖ B is identified with the odd part of  $Y_d' + Y_n'$
- ❖ C is identified with the odd part of  $Y_d' - Y_n'$
- ❖ D is identified with the even part of  $Y_d' - Y_n'$

For a network to be symmetrical it is necessary that its ABCD matrix has A=D

❖ **Step E:**

- Transmission line impedances are extracted from ABCD matrix

$$Z_1 = \frac{A(s)}{C(s)} \Bigg|_{s=1} = \frac{B(s)}{D(s)} \Bigg|_{s=1} \quad (3)$$

- Matrix multiplication is performed resulting new ABCD matrix

$$\frac{1}{1-s^2} \begin{bmatrix} 1 & -Z_1 s \\ \frac{s}{-Z_1} & 1 \end{bmatrix} \begin{bmatrix} A & B \\ C & D \end{bmatrix} = \begin{bmatrix} \bar{A} & \bar{B} \\ \bar{C} & \bar{D} \end{bmatrix}$$

- The new Input Impedance

$$\bar{Z}(s) = \frac{\bar{A} + \bar{B}}{\bar{C} + \bar{D}}$$

The Next line impedance is

$$Z_2 = \left. \frac{\bar{A}(s)}{\bar{C}(s)} \right|_{s=1} \quad (4)$$

In this way all the line impedances may be obtained. Since the structure is symmetrical, it is necessary to perform a cycle of  $(n+1)/2$  times, where,  $n$  is the odd number of section in the line.

The overall transfer matrix for three sections is given by [8]

$$\frac{1}{(1-t^2)^{3/2}} \prod_{r=1}^3 \begin{bmatrix} 1 & Z_r t \\ t/Z_r & 1 \end{bmatrix} = \frac{1}{(1-t^2)^{3/2}} \begin{bmatrix} A(t) & B(t) \\ C(t) & D(t) \end{bmatrix} \quad (5)$$

where,  $t = j \tan \theta$ . In this case  $A(t) = D(t)$  because of the symmetry of the network.

The overall matrix can be expressed as

$$\begin{bmatrix} EP_3(t) & OP_3(t) \\ OQ_3(t) & EQ_3(t) \end{bmatrix} = \prod_{r=1}^3 \begin{bmatrix} 1 & Z_r t \\ -\frac{t}{Z_1} & 1 \end{bmatrix} \quad (6)$$

To obtain the value of  $Z_1$  the overall matrix (6) is pre multiplied by the inverse matrix

$$\frac{1}{(1-t^2)} \begin{bmatrix} 1 & Z_1 t \\ t/Z_1 & 1 \end{bmatrix} \quad (7)$$

and then condition that all elements of the resulting matrix must be divisible by  $(1-t^2)$  is applied.

The overall transfer matrix becomes

$$\frac{1}{(1-t^2)^{3/2}} \begin{bmatrix} at^2 + b & ct^3 + dt \\ et^3 + ft & at^2 + b \end{bmatrix} \quad (8)$$

Pre multiplying (8) by (7) gives the matrix

$$\frac{1}{(1-t^2)^{5/2}} \begin{bmatrix} 1 & Z_1 t \\ t/Z_1 & 1 \end{bmatrix} \begin{bmatrix} at^2 + b & ct^2 + dt \\ et^3 + ft & at^2 + b \end{bmatrix} = \frac{1}{(1-t^2)^{5/2}} \begin{bmatrix} -eZ_1 t^4 + (a - Z_1 c)t^2 + b & (c - aZ_1)t^3 + (d - Z_1 b)t \\ (e - \frac{a}{Z_1})t^3 + (f - \frac{b}{Z_1})t & -\frac{c}{Z_1}t^4 + (a - \frac{d}{Z_1})t^2 + b \end{bmatrix} \quad (9)$$

Since all elements divisible by  $(1-t^2)$  are given by

$$Z_1 = Z_3 = \frac{a+b}{e+f} = \frac{c+d}{a+b} \quad (10)$$

Matrix (9) reduces to

$$\frac{1}{(1-t^2)^{3/2}} \begin{bmatrix} -eZ_1 t^2 - b & (c - aZ_1)t \\ e - \frac{a}{Z_1} & -\frac{c}{Z_1}t^2 - b \end{bmatrix} \quad (11)$$

Repeating this process and pre multiplying (11) by

$$\frac{1}{(1-t^2)} \begin{bmatrix} 1 & -Z_2 t \\ -t/Z_2 & 1 \end{bmatrix}$$

We see that

$$Z_2 = \frac{eZ_1 + b}{\frac{a}{Z_1} - e} = \frac{aZ_1 - c}{\frac{c}{Z_1} + b} \quad (12)$$

In this way, by pre multiplying, the generalized solution may be obtained. So we get the required parameter i.e. all the line impedances values of the coupler.

By the use of MATLAB software we obtain the line impedance values for different ripple value.

These line impedance values are further required to obtain the coupling coefficient values so that we can find the amount of coupling for every element of the coupler. After that, HFSS software is used for designing the coupler.

Table 1.1 Characteristics impedance values for 3-element coupled line

$\delta$	$Z_1$	$Z_2$
0.1	1.2785	3.6702
0.2	1.3978	4.0656
0.3	1.2399	3.5431
0.4	1.2703	3.6656

The coupling coefficient of each section is obtained by

$$C_i = \frac{Z_i^2 - 1}{Z_i^2 + 1}$$

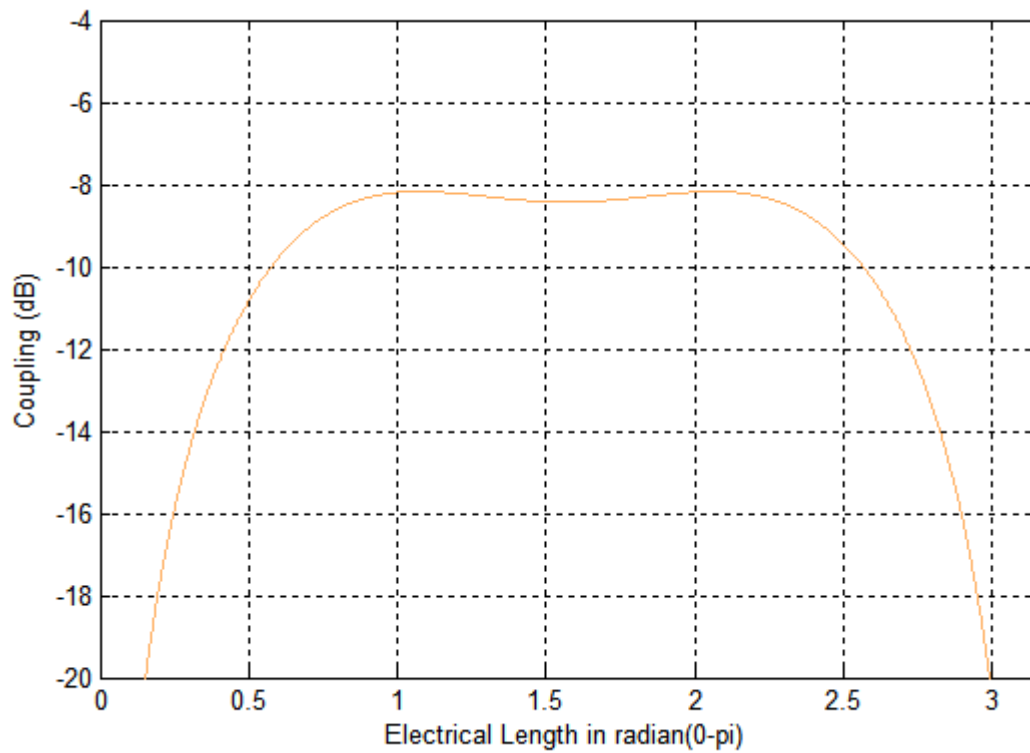


Fig. 1.9 Characteristic of 3-elements, 8.34dB section using table values of crystal.

## CHAPTER 2

### LITERATURE SURVEY

---

In order to find the right topic for the dissertation, various research papers have been studied. The papers related to the selected topic are chosen based on the previous research done and its applicability, and studied thoroughly. Literature survey helps in getting better understanding and learning sustainable approach to carry out the required work.

**Bernard M. Oliver** [1] provided a simple treatment by eradicating the natural coupling since it caused cross-talk. He proposed matrix algebra for the investigations that provided mathematical solutions to the problem. By providing the required change to coupling with distance, variations in transmission characteristics were realized.

**E. G. Crystal *et al.*** [2] designed tables for multi-element couplers, symmetrical in nature, using equal ripple polynomial. The design parameters were developed for different number of elements, viz. three, five, seven and nine, for wide bandwidth. Design tables for these couplers having mean coupling of -3.01, -6 and 8.34 were presented with various equal-ripple tolerances. For the given mean coupling and tolerance, it was shown that couplers of defined number of sections gave maximum bandwidth. Designs for maximally flat coupler were also demonstrated to complete the tables.

**Ralph Levy** [6] gave the designs of two to six section directional couplers. These couplers have an equal ripple approximation to mean coupling and are optimum such that for a specific number of sections maximum bandwidth is available. Thus, synthesis procedure can be derived for multi element directional couplers with different number of elements. The approach was based on the equivalence between the directional coupler and that of a stepped filter.

**Yadav et al** [7] gave a theoretical analysis on junctions and said that it is reactive in nature, i.e., it may either behave capacitive or inductive. Analyses were done and compensation designs were developed for the junction discontinuity effect in multi-element coupled lines. The performance of these couplers was analyzed with the effect of discontinuity in the junction for both inductive and capacitive nature of the junction. The junction behavior can be predicted on the basis of coupling performance and thus, required compensation can be defined for the known behavior of the junction. These theoretical analyses have been proved and verified through 3-D simulation of two different models with different behavior of their respective junctions, in electromagnetic, using HFSS. Based on this analysis, the effect of discontinuity in the junction can be completely compensated.

**P. P Toullos et al.** [8] obtained a composite approach for 3-element and 5-element based on symmetrical coupler. This approach was based on equivalent between directional coupler and stepped filter, as given by Levy and Young. Toullos obtained the results for 5-element coupler and showed the bandwidth improvement over the 3-element coupler and that the result was in good agreement with theoretical response. Also, an experimental model was developed for 5-element coupler having good agreement with the theory and insertion loss function was also obtained for the 5-element coupler which resulted in an equal-ripple response.

**SEYMOUR B. COHN et al.** [13] examined various passive components of microwave, especially the directional couplers. Maxwell theory on electromagnetic wave using the spark-gap microwave source was proved by Hertz until 1930. However, the work in the microwave range remained unknown until then with limited use until 1939. World War II saw the advancement in these passive components because of the needs of military for radar, limitations in space and invention of high power magnetrons. Thus, the paper focused on the sub fields of these directional couplers, rotary joints, transitions from co-axial cable to waveguides, etc.

**K. C. Gupta, Tatsuo Itoh, Arthur A. Oliner** [16] presented the past and future scope of microwave and RF education. Primary events that led to the development of microwave and RF education have been summarized. These events may be listed as

the need for radar during world war-II for the military use, emergence of printed transmission lines during 1950s, invention of integrated circuits and solid-state devices of microwave in the 1960s, the exceeding accessibility of computers and the growth of numerical methods in the 1970s, and the accessibility of circuit simulators and field simulators of microwave in the 1980s and 1990s, respectively. The results and scope of advances in internet technology have also been defined for the dispersal of information. The paper at the end focused on the challenges of microwave and RF engineers.

**I. J. Bahland, K. C. Gupta** [17] In this, the author has discussed about the power handling capacity and gives information about the calculation of rise in temperature of the strip conductor. Electrostatic and the heat flow fields are used for the calculation and also the paper presented the expression for the average power handling ability.

**Yadav et al.** [18] discussed about the analysis of multi-element coupled line with the incorporation of the discontinuity effect and its miniature at the final stage of designing. The design has its applicability in high power RF system. Junctions are basically formed when two elements are connected to each other. Because of the formation of junction, an undesired property comes into effect which can degrade the property of the coupler. These discontinuities are found in VHF frequency because of structural length increase. Design rated for 38-112MHz and power of 200KW has been simulated. The simulation is done on HFSS. The results which are obtained after simulation are highly deviated from the theoretical result in which the effect of discontinuity is ignored.

**Jones et al.** [22] developed the phase and impedance equations for coupled lines of several configurations, one of which is coupled lines with one end connected. Jones and Balljahn also provide equations relating the image impedance, and the image transfer constant.

**J. Reed et al.** [23] analyzed four-arm networks for example double stub coupler and the hybrid coupler, also known as the rat race. In these networks, the wave is divided into even and odd mode. The sum or difference of transmission and reflection

coefficients for the even and odd mode gives the amplitude of a respective arm in the network. A directional coupler with zero decibels expressed and its use as duplexer has also been explained. Multiple stub- coupler designs have been defined for different degrees of coupling and computations of bandwidth curves and output power from different arms are also done. Tables were presented for six 3dB couplers and their characteristics were studied like standing wave ratio, isolation and power splitting with respect to frequency.

**Henry J. Riblet** [24] has given a general solution of the synthesis of equal length impedance transformers with given insertion loss function. It shows that optimum Tchebycheff characteristics can be physically realized and are true optimums for quarter wavelength transformers.

**J.K Shimizu** *et al.* [25] has given the formula for the two basic type the one is quarter wavelength long at the center of its frequency band and the other is three-quarter wavelength long design of coupled transmission line directional coupler. The quarter wavelength type can be used over an octave of frequencies with approximately constant coupling, while the three quarter wavelength type can be used over than two octaves. The experimental results for models of these directional couplers have been found to conform very closely to the theoretical coupling functions, while the directivity is limited by discontinuity effects and constructional tolerances.

**R. Levy** [28] has given the tables for the design of TEM-mode asymmetrical coupled line couplers. In this paper the present computation gives results to only 6 elements. A limitation on n no. of elements will occur because of the accuracy of the computer is limited by the effective number of decimal places to which numbers are held. Synthesis for large number of n would demand better than 9-figure accuracy. In this Levy showed the table for different coupling values for n up to six.

**Person** *et al.* [30] proposed some original technological configurations for implementing highly coupled wideband structures in a 3D environment. Thanks to a convenient combination of thinkable topologies, difficulties commonly encountered with a classical approach can be solved. Different design examples of couplers are

given, and experimental and simulated results are presented.

**R. P. Yadav** *et al.* [37] presented the design of 3dB hybrid coupler of 1.5 MW having frequency 30-96MHz and the applicability of the designing ICRH system. With the increase of power, author takes into consideration various structural parameters related to the design which deteriorates the performance of the coupler. All the parameters like tolerance, discontinuities related to fabrication have been considered and explained theoretically.

### 3.1 Introduction

This chapter gives knowledge about the transmission lines and the development of ultra-wide band 3dB hybrid coupler using these transmission lines. It deals with the basic theory of coupled lines. This helps in governing the type, parameters and configuration of transmission lines as per the application. For high power handling applications, circular rigid transmission line is employed[9, 10]. However, strip line with similar configuration is used for ultra-wide band couple line design.

### 3.2 Review of Transmission Line Theory

A transmission line is a cable or any structure that is designed to carry alternating current of radio frequency such that current and voltage vary in both magnitude and phase over the length. Now, according to the transmission line theory, the physical dimensions of a transmission line network are a fraction of wavelength [38]. When a TEM wave propagates, the transmission line has at least two conductors. Lumped equivalent of the two wire transmission line is shown in Fig. 3.1. (a) and (b), with  $R$ ,  $C$ ,  $L$ ,  $G$  defined as series resistance, shunt capacitance, series inductance and shunt conductance per unit length, respectively.

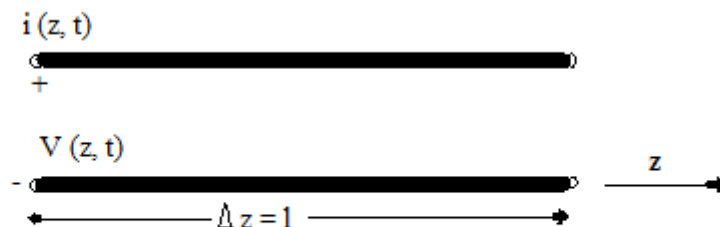


Fig. 3.1(a) Transmission line

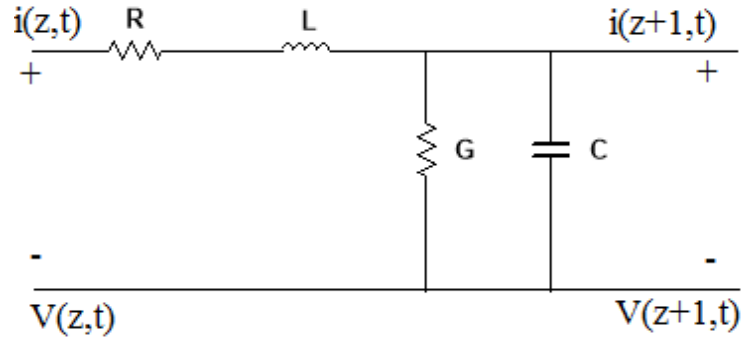


Fig. 3.1(b) Transmission line lumped equivalent circuit

Voltage and current for the TEM wave travelling along the z-direction can be obtained by the given equations [4, 11]:

$$\frac{dV(z)}{dz} = -(R + j\omega L)I(z) \quad (1a)$$

$$\frac{dI(z)}{dz} = -(G + j\omega C)V(z) \quad (1b)$$

$$\frac{d^2V(z)}{dz^2} - \gamma^2 V(z) = 0 \quad (1c)$$

$$\frac{d^2I(z)}{dz^2} - \gamma^2 I(z) = 0 \quad (1d)$$

$$\gamma = \alpha + \beta = \sqrt{(R + j\omega L)(G + j\omega C)} \quad (1e)$$

These equations represent the travelling wave in z-direction which has solution

$$V(z) = V^+ e^{-\gamma z} + V^- e^{\gamma z} \quad (2a)$$

$$I(z) = I^+ e^{-\gamma z} + I^- e^{\gamma z} \quad (2b)$$

where,  $e^{-\gamma z}$  and  $e^{\gamma z}$  represent wave propagation in +z and -z directions respectively. In time domain this can be written as,

$$V(z,t) = V^+ e^{-\alpha z} \cos(\omega t - \beta z) + V^- e^{\alpha z} \cos(\omega t + \beta z) \quad (3a)$$

$$I(z,t) = I^+ e^{-\alpha z} \cos(\omega t - \beta z) + I^- e^{\alpha z} \cos(\omega t + \beta z) \quad (3b)$$

where,  $\alpha$  and  $\beta$  are the attenuation and propagation constant respectively. Applying equation (1a) to the voltage of (1b) gives the current

$$I(z) = \frac{\gamma}{R + j\omega L} [V^+ e^{-\gamma z} + V^- e^{\gamma z}] \quad (4a)$$

On comparing with (2b), we see that characteristic impedance,  $Z_o$  can be defined as

$$Z_o = \frac{R + j\omega L}{\gamma} = \sqrt{\frac{R + j\omega L}{G + j\omega C}} \quad (4b)$$

Also, we find that wavelength  $\lambda$  and phase velocity  $v_p$  can be given as

$$\lambda = \frac{2\pi}{\beta}$$

$$v_p = \frac{\omega}{\beta}$$

This is obtained for a lossy line. In many practical cases, loss of the line can be neglected, resulting in simplification. Substituting  $R=G=0$  for a lossless-line, we have,

$$\gamma = \omega\sqrt{LC},$$

$$\beta = \omega\sqrt{LC}$$

$$\alpha = 0$$

$$Z_o = \sqrt{\frac{L}{C}} \quad (5a)$$

$$\lambda = \frac{2\pi}{\omega\sqrt{LC}} \quad (5b)$$

$$v_p = \sqrt{\frac{1}{LC}} \quad (5c)$$

### 3.2.1 Choice of Transmission Lines

A transmission line is characterized by the values of capacitance and inductance distributed along the network length. In coaxial transmission line, the electromagnetic field is confined between the inner and the outer conductor and supports TEM mode which has no cut off. Thus, it may be employed from very low to very high frequencies [35]. A coaxial transmission line, even though it has very good power handling capability, cannot be employed in ultra-wide band devices because of its non-planer structural configuration. It is thus necessary to have a transmission line which is compatible for designing complex structure of ultra-wide band hybrid coupler. This is realized by planar strip line type transmission line. The first planar transmission line called the strip transmission line was proposed by Barrett and Barnes [12] as early as in 1951. The structure has a thin strip conductor surrounded by a rectangular outer conductor. Although it is somewhat similar to coaxial transmission line, but has many advantages over it, such as, compact size, simple geometry, easy fabrication and suitability in the development of ultra-wide band devices.

Also, many other configurations of the planar transmission line were proposed later from the year 1952 to 1970 like micro strip line, slot line, suspended micro strip, suspended strip line, inverted micro strip, co-planar waveguide and co-planar strip [13]. Unlike the strip line, these transmission lines are limited to the low power applications and require a dielectric substrate of very high permittivity to confine the electromagnetic field near the strip conductor. Therefore, 3dB hybrid coupler concept based on strip line is selected for simple and cost effective design and for the ease of fabrication.

### 3.2.2 Strip line

The transverse electromagnetic mode (TEM) is the dominant mode of propagation in the strip line and has radial electric field and azimuthal magnetic field. TEM wave has phase velocity  $v_p$ , propagation constant  $\beta$  and  $Z_o$  characteristic impedance, given by

$$v_p = \frac{c}{\sqrt{\epsilon_r}}$$

$$\beta = \frac{\omega}{v_p} = \omega\sqrt{\mu\epsilon}$$

$$Z_o = \sqrt{\frac{L}{C}} = \frac{\sqrt{LC}}{C} = \frac{v_p}{C}$$

where,  $c$  is the velocity of light in free space and  $\epsilon_r$  is relative permittivity of the dielectric between the conductors.  $L$  and  $C$  are the inductance and capacitance per unit length of the line where,  $C$  can be evaluated in following different ways:

1. Conformal mapping techniques,
2. Mode matching techniques,
3. Finite difference and finite element solutions.

The resulting solutions of these methods involve complicated functions and thus, simple formulae are used for practical computations. The two well-known approximations are given as,

- Hawe's Approximation Formula [14]:

$$Z_o = \frac{30\pi}{\epsilon_r} \left( \frac{b}{w_e + 0.441b} \right)$$

where,  $w_e$  is the effective width of the center conductor

$$\frac{w_e}{b} = \frac{w}{b} - \begin{cases} 0 & \text{for } \frac{w}{b} \geq 0.35 \\ \left(0.35 - \frac{w}{b}\right)^2 & \text{for } \frac{w}{b} \leq 0.35 \end{cases}$$

It is assumed here that thickness  $t=0$ . We see that the accuracy is 1% of the exact results and that  $Z_o$  decreases as  $w$  increases. While designing strip line circuit, we need  $w$ , whereas  $Z_o$ ,  $b$  and  $\epsilon_r$  are given.

- Collin's Approximate Formula [15]:

$$Z_o = \begin{cases} \frac{\pi\eta_o}{8\sqrt{\epsilon_r} \left( \ln 2 + \pi \frac{2}{2b} \right)} & \text{for } w \geq 0.2b \\ \frac{\eta_o}{2\pi\sqrt{\epsilon_r}} \ln \left( \frac{8b}{\pi w} \right) & \text{for } w \leq 0.2b \end{cases}$$

If we denote the attenuation constant due to the center conductor as  $\alpha_{c1}$  and the attenuation constant due to ground planes as  $\alpha_{c2}$ , then we have the following approximate formulas:

$$\alpha_{c1} = \frac{R_s \sqrt{\epsilon_r} \ln \left( \frac{4b}{\pi T_e} \right) \frac{\pi w}{2b}}{b \eta_o \ln 2 + \frac{\pi w}{2b}} \quad \text{for } w \geq 0.2b$$

$$\alpha_{c2} = \frac{\pi R_s \sqrt{\epsilon_r} w}{4b^2 \eta_o \left( \ln 2 + \frac{\pi w}{2b} \right)} \quad \text{for } w \geq 0.2b$$

$$\alpha_{c1} = \frac{2R_s \sqrt{\epsilon_r} \ln \left( \frac{4\pi}{T_e} \right)}{\pi w \eta_o \ln \frac{8b}{\pi w}} \quad \text{for } w \leq 0.2b$$

$$\alpha_{c2} = \frac{R_s \sqrt{\epsilon_r}}{\eta_o \left( \frac{8\pi}{w} \right)} \quad \text{for } w \leq 0.2b$$

where,  $T_e = e^{\frac{\pi}{2}} \sqrt{\frac{4wt}{\pi}}$  and  $R_s = \sqrt{\frac{w\mu}{2\sigma}}$

Both these formulae give approximately the equal results. By using these formulae, dimensions of the strip line can be calculated for the given impedance.

## **Power Handling Capability of Strip line**

Dielectric breakdown in a strip line limits its peak power handling capability like any other transmission line. However, increase in temperature due to conductor loss and dielectric loss limits its average power rating.

### **Peak Power Handling Capability**

Peak power handling capability in a strip line depends on the maximum voltage applied without causing any dielectric breakdown. For the maximum voltage  $V_o$  that a strip line of characteristic impedance  $Z_o$  can withstand, maximum peak power  $P_p$  is given by

$$P_p = \frac{V_o^2}{2Z_o}$$

The region between inner to ground conductor can support very high voltage values. Also, maximum electric field on the surface of strip line conductor should be less than the breakdown strength of dry air, which is 30kV/cm at the atmospheric temperature and pressure. Thus, allowances are a must for changes with altitude, humidity and presence of dust particles in the air since this has no margin of safety.

### **Average Power handling Capability**

Increase in temperature in the strip line conductor and dielectric losses determine the average power handling capability. Following parameters are important while calculating average power handling capability [16]:

1. Transmission line losses.
2. The thermal conductivity of the dielectric strip conductor.
3. Surface area of the dielectric strip conductor.
4. Maximum allowable temperature of the strip line structure.
5. Ambient temperature

Heat is generated in the strip line due to loss of electromagnetic power in the strip conductor and the dielectric medium. The heat flows to the ground because the ground plane of the strip line configuration is held at ambient temperature and the

heat is uniformly distributed along the width of the conductor because of good conductivity of the strip metal. This heat flow can be calculated by considering the electric field distribution [17].

The temperature rise  $\Delta T$  of inner conductor with respect to the outer conductor can be determined by the following relation.

$$\Delta T = \frac{P_c + P_d}{G_t}$$

where,  $P_c$  and  $P_d$  represent the dissipation per unit length of the line due to the losses in inner conductor and dielectric respectively;  $G_t$  represent the thermal conductance of the strip conductor.  $P_c, P_d$  and  $G_t$  can be expressed as

$$P_c = 2\alpha_c P_T$$

$$P_d = 2\alpha_d P_T$$

$$G_t = \frac{120\pi g}{Z_o \sqrt{\epsilon_r}}$$

where,  $P_T$  is incident power in watts,  $\alpha_c$  and  $\alpha_d$  are loss coefficients of the conductor and dielectric (neper per unit length),  $g$  is thermal conductivity of the dielectric medium and  $Z_o$  is characteristic impedance of the stripline.

Substituting these in  $\Delta T$  above, we obtain:

$$\Delta T = \frac{(\alpha_c + \alpha_d)Z_o \sqrt{\epsilon_r} P_T}{60\pi g}$$

That means that the temperature rise  $\Delta T_{perwatt}$  per one watt of incident power is,

$$\Delta T_{perwatt} = \frac{(\alpha_c + \alpha_d)Z_o \sqrt{\epsilon_r}}{60\pi g} C/W$$

### **Maximum Average Power Handling Capability:**

Maximum average power that a strip line can handle is given by [17]:

$$P_{av} = \frac{T_{max} - T_{amb}}{\Delta T_{perwatt}}$$

It is defined as the maximum power that a strip line can handle with rise in temperature from  $T_{amb}$  to  $T_{max}$ .

Here,  $T_{max}$  is the maximum operating temperature,  $T_{amb}$  is temperature of the outer conductor and  $\Delta T$  denotes rise in temperature per watt. Change of substrate properties and change of physical dimensions with temperature limit the allowable maximum operating temperature of the strip line circuits. The maximum operating temperature of a strip line circuit is the one at which its electrical and physical properties are within the acceptance limits. For example, the maximum temperature of polystyrene is found to be  $100^{\circ}C$ . So, the breaking point of  $T_{max}$  is taken as  $100^{\circ}C$  in this case. Hence, the maximum allowable temperature can be safely limited to  $100^{\circ}C$  for average power handling calculations.

## Comparison between Single Element and Multi-element Coupled Lines

---

### 4.1 Introduction

This chapter describes the comparison of single element and multi element coupled lines. We have already studied that single element coupler has narrow bandwidth compared to multi element coupler. This has been proved by graphical analysis using mathematical tool below.

Coupled lines are formed if there are two transmission lines close enough such that power is transferred from one transmission line to other transmission line. Single element coupled line means having a quarter wavelength coupled line and having a limited application due to the desired bandwidth available. It works in a narrow frequency band, but the bandwidth can be increased substantially by connecting several sections of quarter wavelength coupled elements in a certain configuration called multi-element coupler.

The comparison is based on 8.34dB of single section and then multiple sections of three sections, five sections and seven sections. We have compared the results of single and multiple sections and found that the results are in good agreement to the theory. The overall coupling of  $8.34 \pm 0.2dB$  for single, three, five, seven elements coupled lines section using Crystal tabulated parameter is analyzed and plotted using MATLAB software as shown in Fig.4.2,4.3, 4.4 and 4.5.

Parameter like characteristic impedance ( $Z_1, Z_2 \dots$ ) is taken from crystal tabulated data.

Appropriate values of coupling coefficient ( $C_1, C_2, \dots, C_N$ ) for the desired coupling response of ultra-wide band coupler can be calculated as

$$C_N = \frac{Z_N^2 - 1}{Z_N^2 + 1}$$

## 4.2 For Single Coupled line section

The ratio of voltage at coupled port to voltage at input port is given by [5]

$$\frac{V_3}{V_1} = \frac{jC \tan \theta}{\sqrt{1-C^2} + j \tan \theta}$$

$$\frac{V_3}{V_1} = \frac{jC \tan \theta}{1 + j \tan \theta} = jC \sin \theta e^{-j\theta}$$

This ratio gives us the desired coupling with  $C \ll 1$

Also, the ratio of voltage at output port to the voltage at the input port is given by [5]

$$\frac{V_2}{V_1} = \frac{\sqrt{1-C^2}}{\sqrt{1-C^2} \cos \theta + j \sin \theta}$$

$$\frac{V_2}{V_1} = e^{-j\theta}$$

By calculating  $C \ll 1$  equal to 0.38 we get the result approx. to 8.34dB for the single section coupler. The coupling versus electrical length plot has been plotted by using the MATLAB as shown in Fig. 4.1 below.

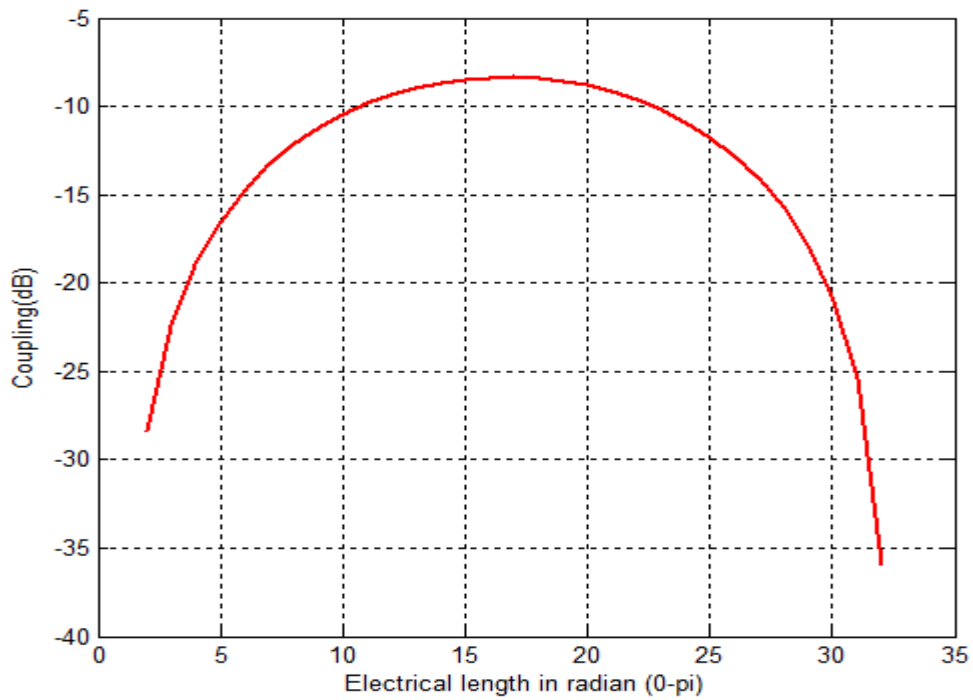


Fig.4.1 Characteristic of single-element, 8.34dB coupled line section

The graph shows that single section coupler has a narrow range of frequency for the desired band.

### 4.3 For Multi-element Coupled line section

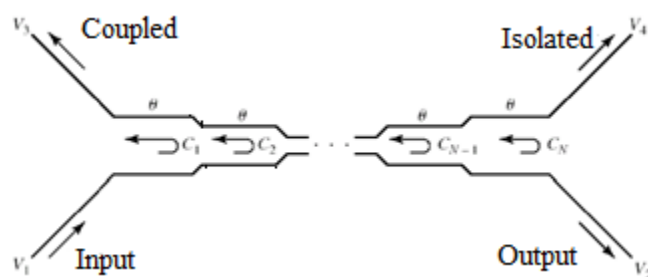


Fig. 4.2 N-section multi-element coupler

The multi-section analysis has also been done similar to single section as follows:

The total voltage at coupled port of the cascaded coupler can be expressed as [5],

$$V_3 = (jC_1 \sin \theta e^{-j\theta})V_1 + (jC_2 \sin \theta e^{-j\theta})V_1 e^{-2j\theta} + \dots + (jC_N \sin \theta e^{-j\theta})V_1 e^{-2j(N-1)\theta}$$

$$V_3 = 2jV_1 \sin \theta e^{-jN\theta} \left[ C_1 \cos(N-1)\theta + C_2 \cos(N-3)\theta + \dots + \frac{1}{2}C_M \right]$$

where,  $M = \left( \frac{N+1}{2} \right)$  with N is the number of sections cascaded

At the center frequency, we define the voltage coupling factor  $C_o$

$$C_o = \left. \frac{V_3}{V_1} \right|_{\theta=\pi/2}$$

### 4.3.1 Three-Element Coupled line section

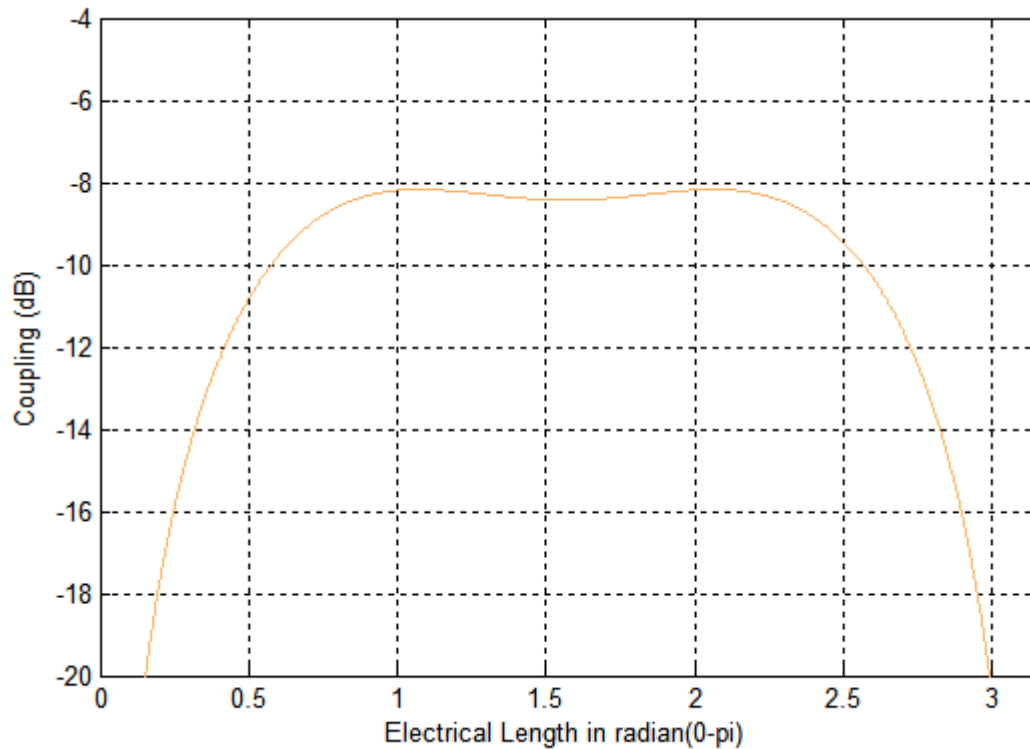


Fig. 4.3 Characteristic of 3-elements, 8.34dB coupled line section using Cristal theory

The above figure shows the coupling between 3-elements for  $8.34 \pm 0.2dB$ , which uses the Crystal tabulated parameters having

$$Z_1 = 1.0743 \quad Z_2 = 1.7848$$

### 4.3.2 Five-Element Coupled line section

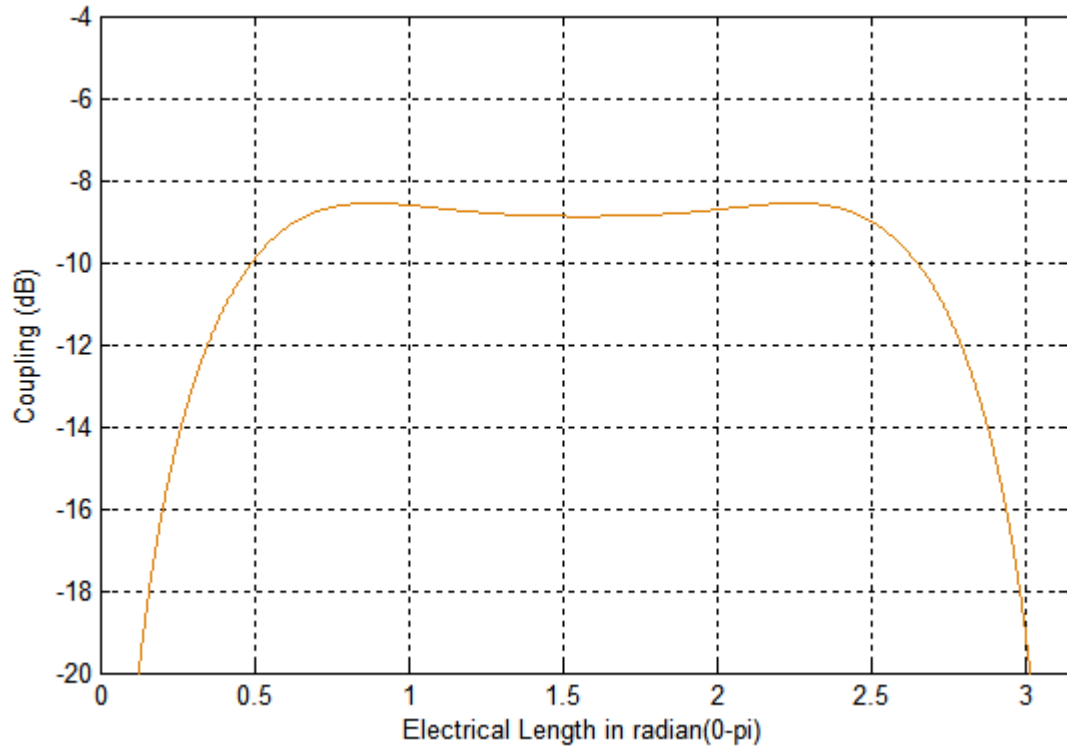


Fig. 4.4 Characteristic of 5-elements, 8.34dB coupled line section using Cristal theory

The above figure shows the coupling between 5-elements for  $8.34 \pm 0.2dB$  which uses the Crystal tabulated parameters with

$$Z_1 = 1.054 \quad Z_2 = 1.1202 \quad Z_3 = 1.8700$$

### 4.3.3 Seven-Element Coupled Line Section

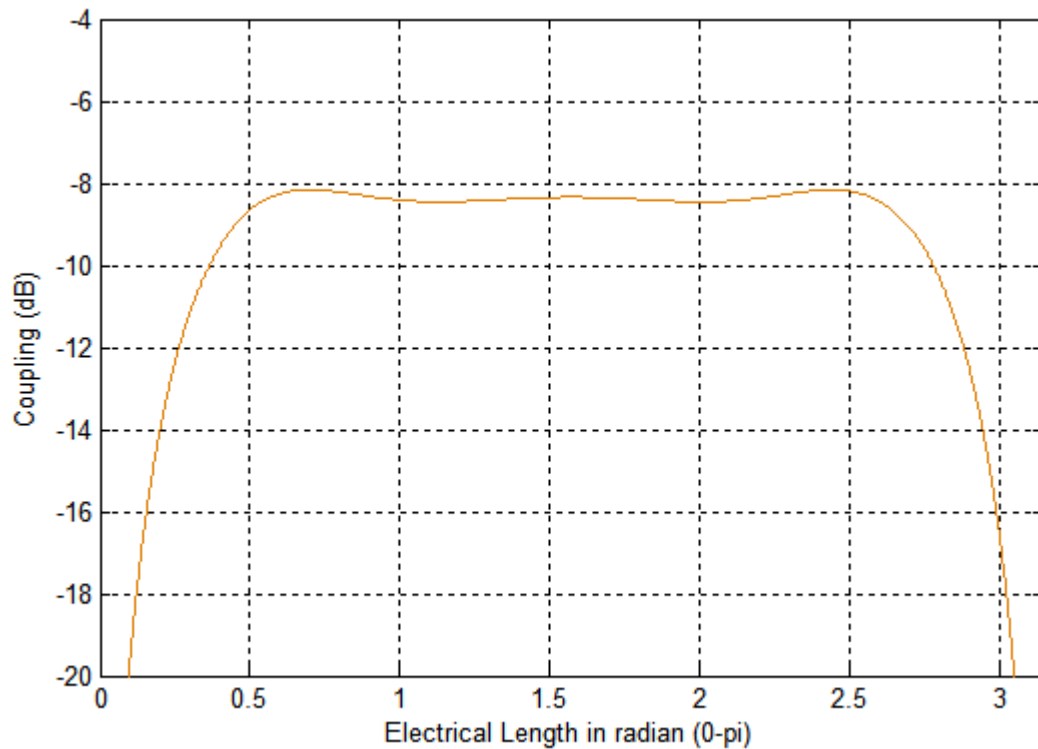


Fig. 4.5 Characteristic of 7-elements, 8.34dB coupled line section using Cristal theory

The above figure shows the coupling between 5-element for  $8.34 \pm 0.2dB$  which uses Cristal tabulated parameters having

$$Z_1 = 1.0046 \quad Z_2 = 1.0440 \quad Z_3 = 1.18141 \quad Z_4 = 2.1209$$

From the above graphical analysis we find that single element has a narrow band as compared to three, five and seven section coupler. For multi element coupler as we increase the number of elements i.e as the number of elements cascaded increases the bandwidth goes on increasing and we get broad bandwidth in multi-element coupler as compared to the single element coupler.

## Design of 3dB Tandem Hybrid Coupler with Single Element

---

### 5.1 Introduction

The design of 3dB Tandem coupler is done by connecting two 8.34dB coupled lines which are aligned one over the other such that the input is equally divided into the coupled and output port with a  $90^{\circ}$  phase difference between them. These outputs can thus drive two antennae simultaneously in the known phase. The 3dB tandem hybrid coupler is used to provide the essential protection to the RF generator. The 3dB hybrid coupler is a 4-port device in which the RF power at input port (port-1) is equally divided between the output port and the coupled port with a phase difference of  $90^{\circ}$  and the port-4 remain isolated [37]. The total reflected power from both port 2 and 3 that are equal in magnitude and phase goes to port 4 which is isolated. Thus, RF generator is protected from the reflected power [18]. The 3dB tandem hybrid coupler can also be used as power divider, combiner and to protect generator by coupling of reflected power to the isolated port. The 3dB coupler is fundamental part of the RF system like cellular communication, broadcast, satellite communication, defense, aerospace etc. It also has several useful applications in the plasma related experiments [19].

In this Chapter, design of strip line based arched type of 50W 3dB Hybrid coupler at 182.5MHz is introduced. Electromagnetic analysis software (HFSS) is used for designing of 3dB hybrid coupler.

In a multi element coupler, for designing 3dB coupler of three-elements, high coupling of nearly 0.5dB is required for the middle section which is difficult to achieve because of very thin gap between the two transmission lines and thus the designing and fabrication of such coupler becomes impractical.

To achieve the wider spacing for designing the 3dB coupler, two 8.34dB quarter wavelength coupled lines are used in tandem. This 3dB coupler can be used as power dividers, combiners and to protect the RF generator from the reflected power [36].

Power handling, frequency of an arched type is selected such that it may be useful in application related to plasma experiments.

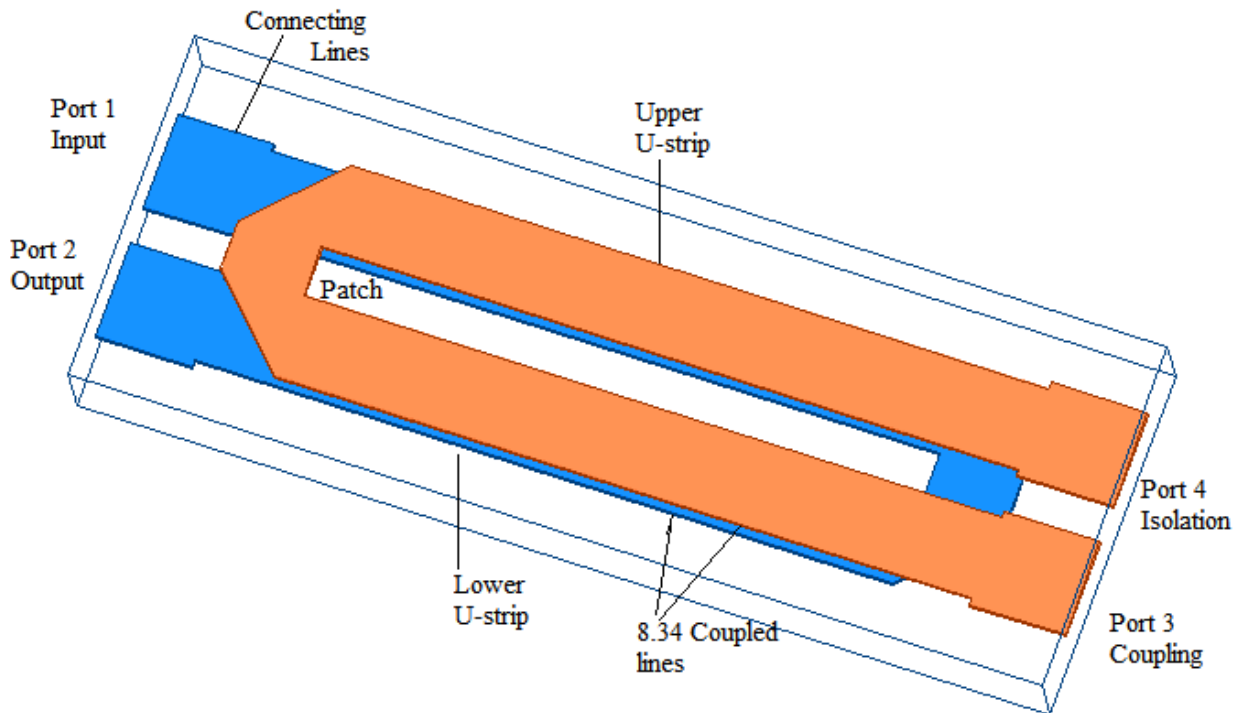


Fig. 5.1 Tandem 3dB hybrid Coupler

## 5.2 Concept and Design of 3dB Tandem Hybrid Coupler

The 3dB tandem coupler consists of metallic enclosure within which two rectangular strip-line central conductors are arranged one over the other as shown in Fig. 5.1.

Coupler model consists of two sections:

1. Coupled section.
2. Non-Coupled section.

The electrical length of the coupled line is taken as quarter wavelength at desired frequency with  $Z_{ce}$  and  $Z_{co}$  as the characteristic impedance for even and odd modes respectively.

The degree of coupling is decided by the width and the gap between the coupled lines. Connecting signal lines and patch of  $Z_o$  characteristic impedance are part of non-coupled section. Patch is used to connect two 8.34dB sections in tandem as patch

is a small segment of strip line. Grounded metallic enclosure filled with air which acts as a dielectric.

### 5.2.1 Coupled Strip-line design

The schematic diagram of single 8.34dB tandem hybrid coupler broad-side coupled strip line is illustrated in Fig. 5.2.

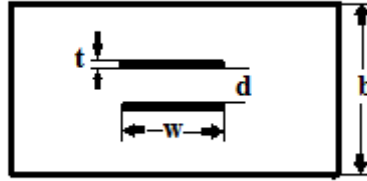


Fig. 5.2 Simplified diagram of Single 8.34dB Coupled strip-line

In the diagram  $b$ ,  $d$ ,  $t$ ,  $w$  define the height of grounded box, spacing between the coupled lines, thickness and width of the coupled lines, respectively.

$Z_{ce}$  and  $Z_{co}$  are the coupled line characteristic impedances of even and odd modes, respectively.

$$Z_{ce} = Z_o \sqrt{\frac{1 + C_v}{1 - C_v}}$$

$$Z_{co} = Z_o \sqrt{\frac{1 - C_v}{1 + C_v}}$$

$$Z_o = \sqrt{Z_{ce} Z_{co}}$$

In order to calculate the parameters we have used following equations given by Cohn [13]

$$Z_{ce} = \frac{59.952\pi}{\sqrt{\epsilon_r}} \frac{K(k')}{K(k)}$$

$$Z_{co} = \frac{94.172\pi d/b}{\sqrt{\epsilon_r \tanh^{-1}(k)}}$$

$$\text{where, } k = \left[ 1 - \left( \frac{0.5 \exp^{\frac{\pi K(k)}{K(k')} - 1}}{0.5 \exp^{\frac{\pi K(k)}{K(k')} + 1}} \right)^4 \right]^{1/2}$$

$$\frac{w}{b} = \frac{2}{\pi} \left[ \tanh^{-1} \sqrt{\frac{k - \frac{d}{b}}{1 - k \frac{d}{b}}} - \left( \frac{d}{b} \right) \tanh^{-1} \sqrt{\frac{k - \frac{d}{b}}{k \left( 1 - k \frac{d}{b} \right)}} \right]$$

where  $k' = \sqrt{1 - k^2}$ ,

$K(k')$  and  $K(k)$  are the complete elliptic integrals of first kind.

The value of  $K(k')/K(k)$  can be found in [20]

All the parameters are found to be as follows:

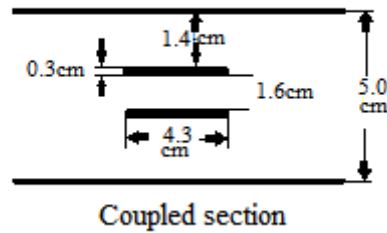


Fig. 5.3 Dimentions of the coupled line section

### 5.2.2 Non-Coupled Strip-line design

Connecting lines and the patch both are the part of non-coupled section. Connecting lines are 0.8cm away from the center, therefore  $2d = 1.6\text{cm}$ ,  $b = 5.0\text{cm}$ ,  $w = 5.0\text{cm}$ ,  $t = 0.3\text{cm}$ . Using these dimensions and by connecting non coupled section to the

coupled one, a tandem 3dB hybrid coupler is obtained. Performance is calculated in terms of S-parameters. Designed dimensions are shown in Fig.5.4.

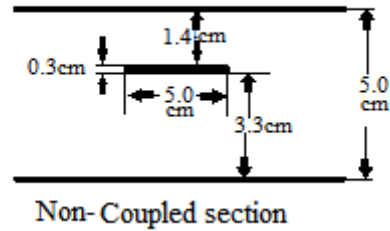


Fig. 5.4 Dimensions of the Non-coupled line section

Both the coupled and non-coupled section are joined in tandem to form a 3dB tandem hybrid coupled section. Performance has been calculated in terms of S-parameters by using HFSS software. HFSS designed results are shown below:

### 5.3 Calculated S-Parameters for Single-element 3dB Tandem Hybrid Coupler.

#### 1. Return loss:-

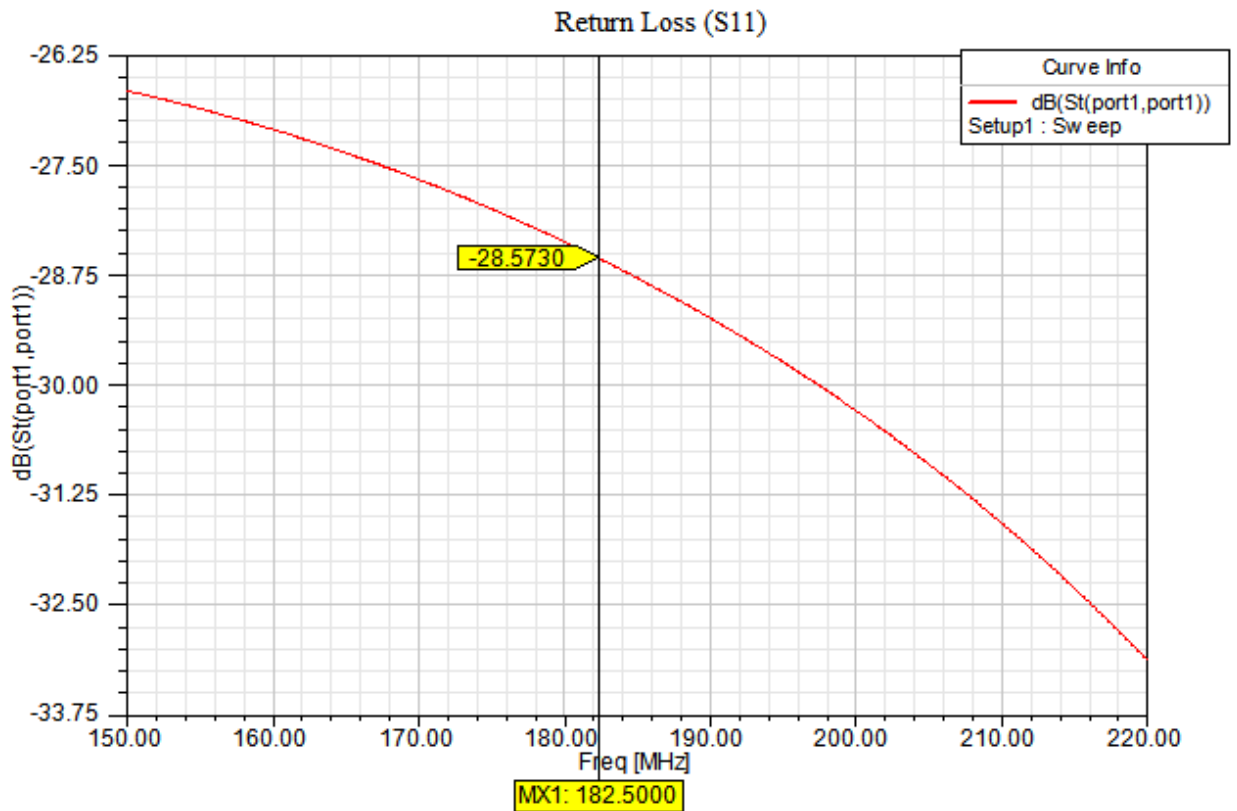


Fig.5.5 Return Loss of 3dB tandem hybrid coupler

The return loss represented as  $S_{11}$  determine how much power is reflected back to port1. At the center frequency of 182.5MHz, the return loss is calculated to be -28.57dB which is approximately .17 % of the input power.

## 2. Output power:-

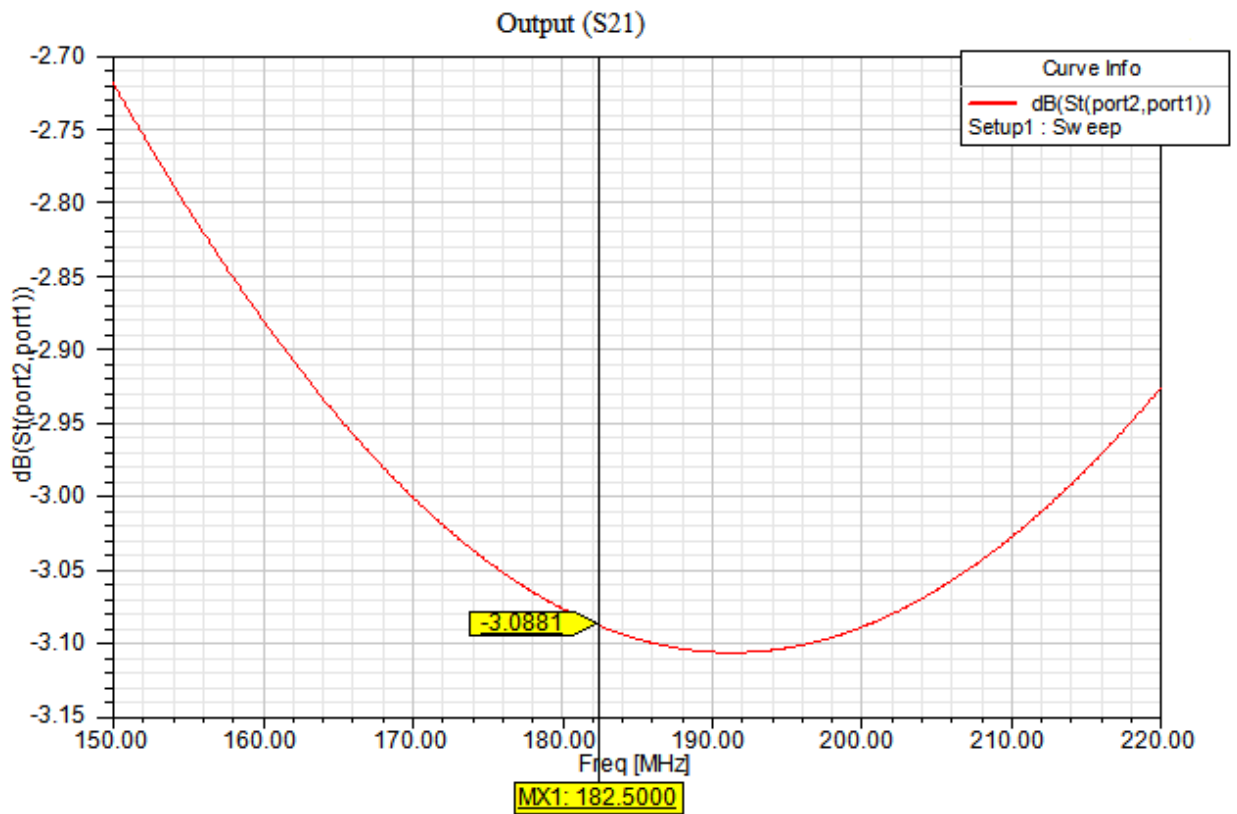


Fig. 5.6 Output of 3dB tandem hybrid coupler

The output represented as  $S_{21}$  determine how much power is received at the output port when input power is given at port1. At the center frequency of 182.5MHz, the output is calculated to be -3.088dB which is approximately 50 % of the input power.

### 3. Coupling power:-

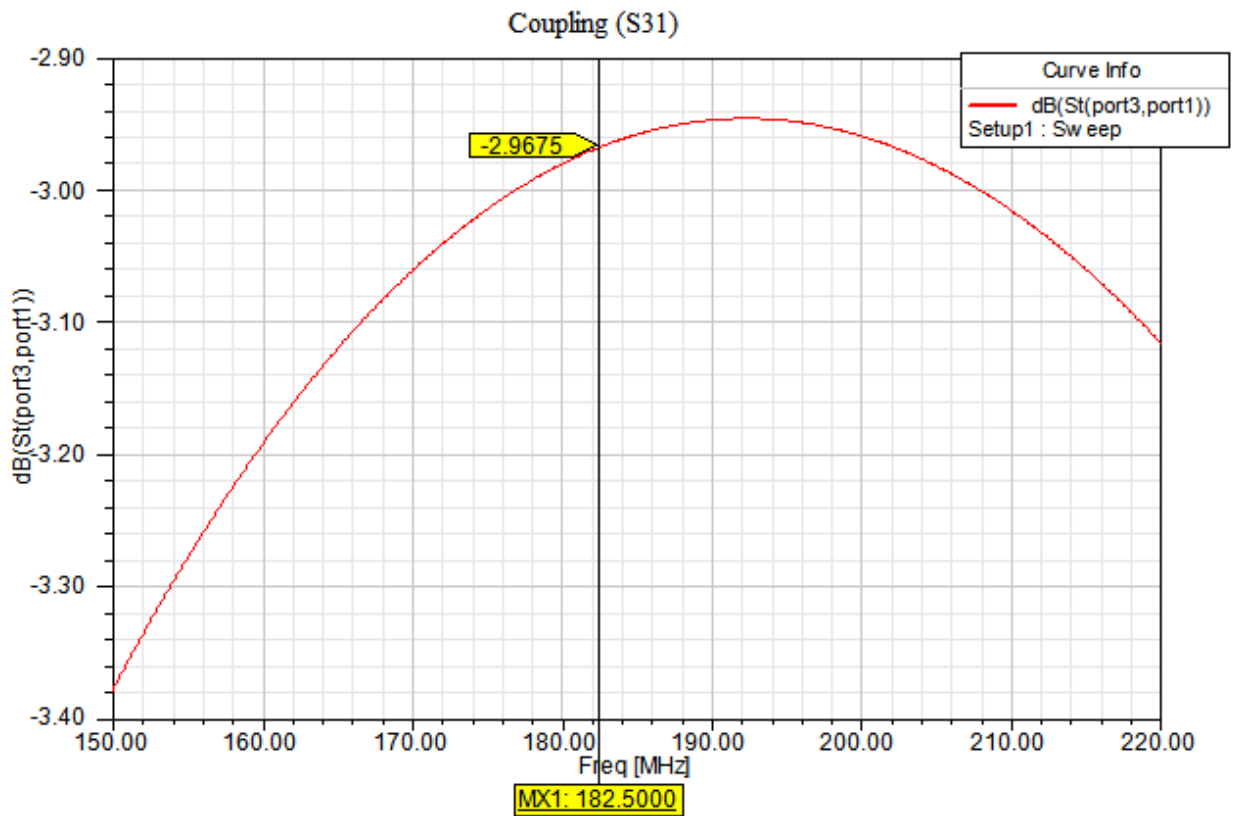


Fig. 5.7 Coupling of 3dB tandem hybrid coupler.

The coupling represented as  $S_{31}$  determine how much power is coupled to port3 from input port. At the center frequency of 182.5MHz, the coupling is calculated to be -2.97dB which is approximately 50 % of the input power.

#### 4. Isolation:-

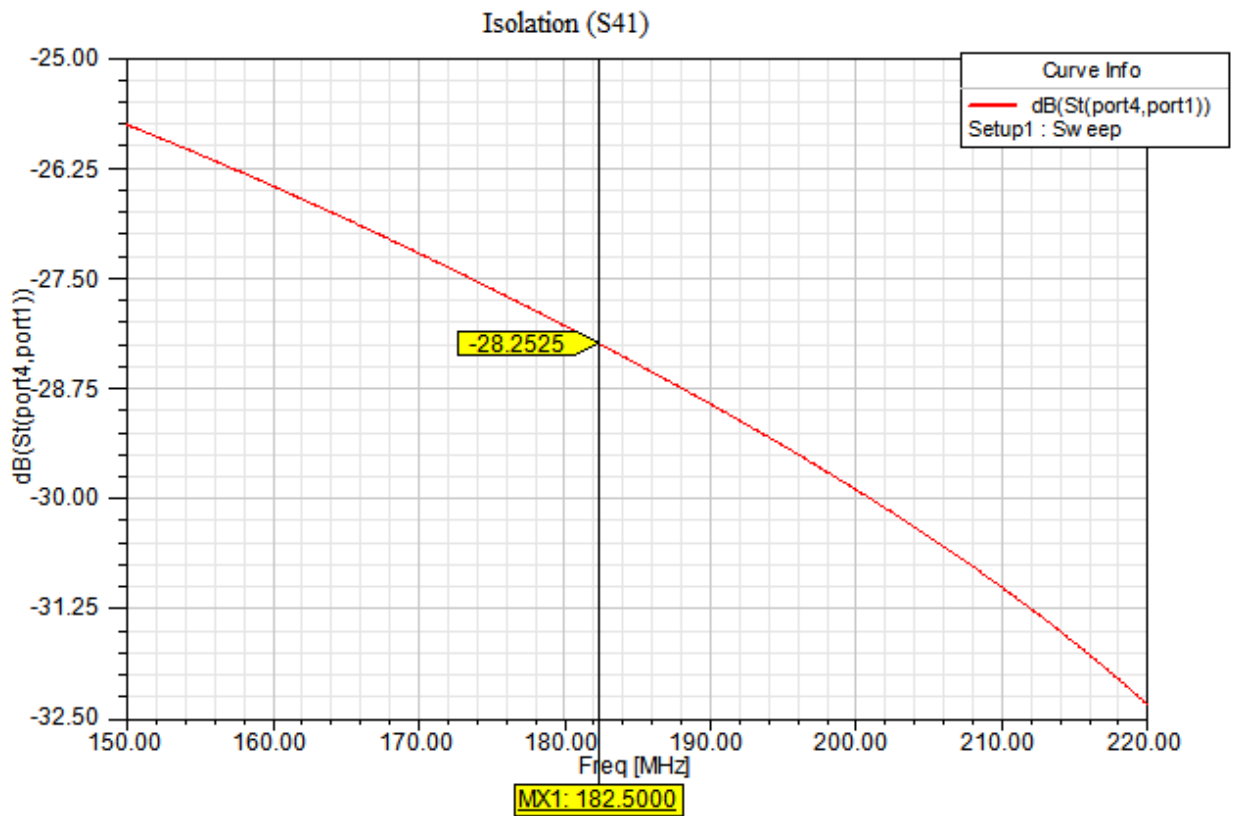


Fig 5.8 Isolation of 3dB tandem hybrid coupler.

Isolation is defined as the difference in signal level between the input port and the isolated port when the other two ports are terminated by the matched load. At the center frequency of 182.5MHz, the isolation is calculated to be -28.25dB which is approximately .18 % of the input power.

## Design of 3dB Tandem Hybrid Coupler with Multi- Elements

### 6.1 Introduction

In the previous chapter, analysis of 3dB hybrid coupler with single element is discussed. Single element coupler works in narrow band of frequency and has limited applications. So, we designed an ultra-wide band 3dB hybrid coupler with multi-element. To increase the bandwidth we cascade multiple section of quarter wavelength so that the coupler works in ultra-wide band frequency.

The designing of 50 Watt 3dB tandem coupler of three sections at 182.5MHz is done by connecting two 8.34dB three section coupled lines which are aligned one over the other such that the input is equally divided into the coupled and output port with a  $90^{\circ}$  phase difference between them.

The 3dB hybrid coupler is a 4-port device in which the input RF power at input port (port-1) is equally divided between the output port (port-2) and the coupled port (port-3) with a phase difference of  $90^{\circ}$  and the port-4 remain isolated. The total reflected power from both port 2 and 3 that are connected to antennae having equal magnitude and phase goes to port 4 which is isolated. Thus, RF generator is protected from the reflected power. The 3dB tandem hybrid coupler can also be used as power divider, combiner and to protect generator by coupling of reflected power to the isolated port.

The two section of 8.34dB coupling with three element are combined in tandem to form 3dB tandem hybrid coupler. Diagram of the symmetrical 8.34dB 3-element coupler is shown in Fig. 6.1, where extreme elements are identical. These three elements are named as B, A, B, where  $A_1, A_2, A_3, A_4$  and  $B_1, B_2, B_3, B_4$  are the return loss, output, coupling and isolation of element-A and element-B, respectively.

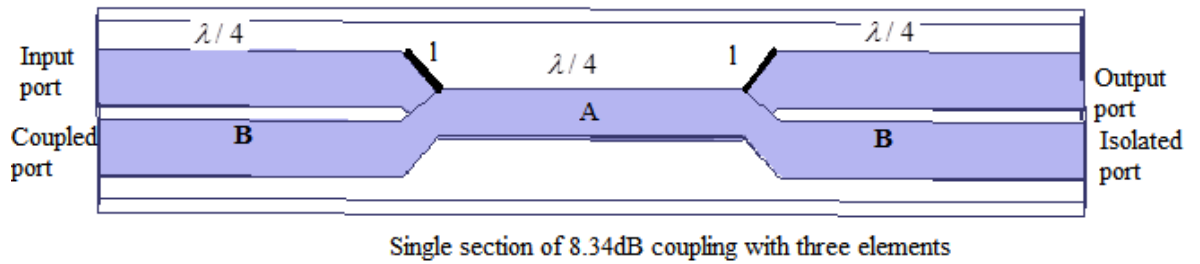


Fig. 6.1 Symmetrical 8.34dB coupled section with three elements.

Every section is having  $\lambda/4$  length section as represented in the figure and junction of length  $l$  is placed to join the two sections. To achieve the exact voltage standing wave ratio and isolation properties, every element has the identical effective characteristic impedance.

$$\sqrt{Z_{0eA} Z_{0oA}} = \sqrt{Z_{0eB} Z_{0oB}}$$

where,  $Z_{0eA}$ ,  $Z_{0oA}$  and  $Z_{0eB}$ ,  $Z_{0oB}$  are the normalized even and odd mode impedances of element-A and element-B respectively.

Fig. 6.2 shows the dimensions of element-A and element-B of one section of 8.34dB coupled three section coupler

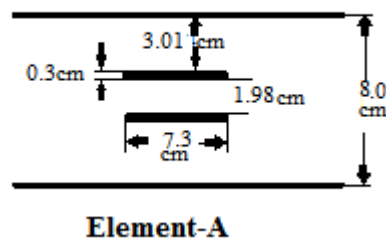


Fig. 6.2(a) Dimensions of Element-A

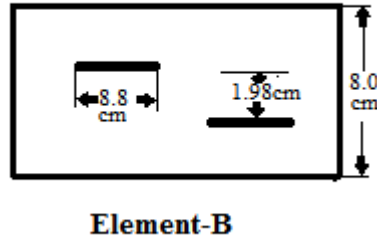


Fig. 6.2(b) Dimensions of Element-B

Crystal [20] table for  $8.34 \pm 0.2dB$  helps in simulation using HFSS, where we get the normalised even mode impedances for three element coupled line as  $Z_{oeA} = 1.7848$  and  $Z_{oeB} = 1.07434$  where  $Z_{oeA}$  is the normalized even mode impedance for element-A and  $Z_{oeB}$  is the normalized even mode impedance for element-B.

After that, the next step is to find the coupling coefficient of element-A and element-B. The coupling coefficient of an element is given by:

$$C_A = \frac{Z_{oeA}^2 - 1}{Z_{oeA}^2 + 1}$$

$$C_B = \frac{Z_{oeB}^2 - 1}{Z_{oeB}^2 + 1}$$

By calculating the values using (1) and (2), the coupling coefficient for element-A and element-B come out to be  $C_A = 0.5222$  and  $C_B = 0.07074$  and the values in Decibel after calculation are found to be:

$$C_A (dB) = -6.123$$

$$C_B (dB) = -22.896$$

The design in HFSS requires dimensions that are calculated for  $C_A$  and  $C_B$  using equation [2, 21]. To join the three elements a junction of length  $l$  is employed and simulation has been performed using HFSS.

Fig. 6.1 shows the model of  $8.34 \pm 0.2\text{dB}$  coupled section consisting of three cascaded section. To achieve the overall coupling of 3dB, similar two section of 8.34dB coupled section are connected in tandem as shown in Fig. 6.3.

## 6.2 Simulation using HFSS of 3dB tandem three element coupler

A metallic Box having dimensions  $179.3\text{cm} \times 65\text{cm} \times 8\text{cm}$  is taken with air inside which acts as a dielectric. Rectangular strip line central conductors are arranged in this metallic box. The length of each element is taken to be  $\lambda/4$  (i.e. 41.1cm) for centre frequency of 182.5MHz. To simulate a 3dB hybrid coupler using HFSS the procedure is described as follows:

The first step is to design element-A and element-B independently and the coupling parameters are to be verified at the centre frequency of 182.5MHz. For element-A, -6.123dB and element-B, -22.896 of coupling is to be verified by HFSS. Simulated coupling result for element-A and element-B are given in Fig. 6.3.(a) and Fig. 6.3.(b).

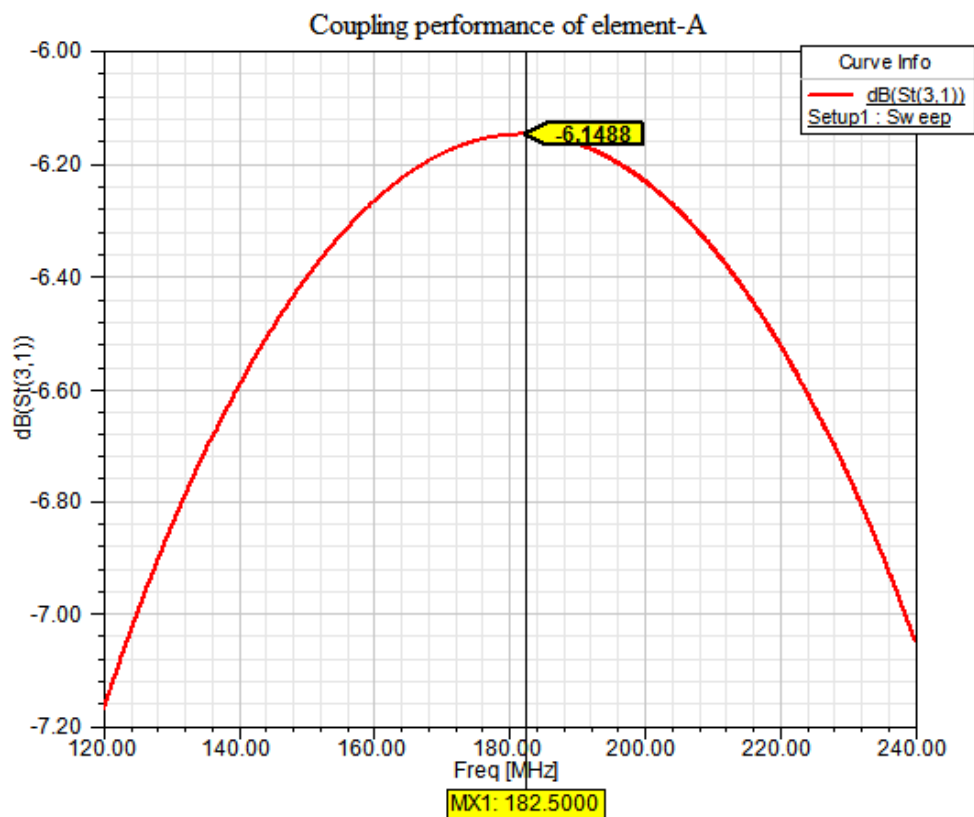


Fig. 6.3(a) Simulated result of Coupling for element-A using HFSS

The result shown in figure shows that at the centre frequency of 182.5MHz the coupling coefficient is nearly equal to the desired coupling of  $-6.123\text{dB}$ .

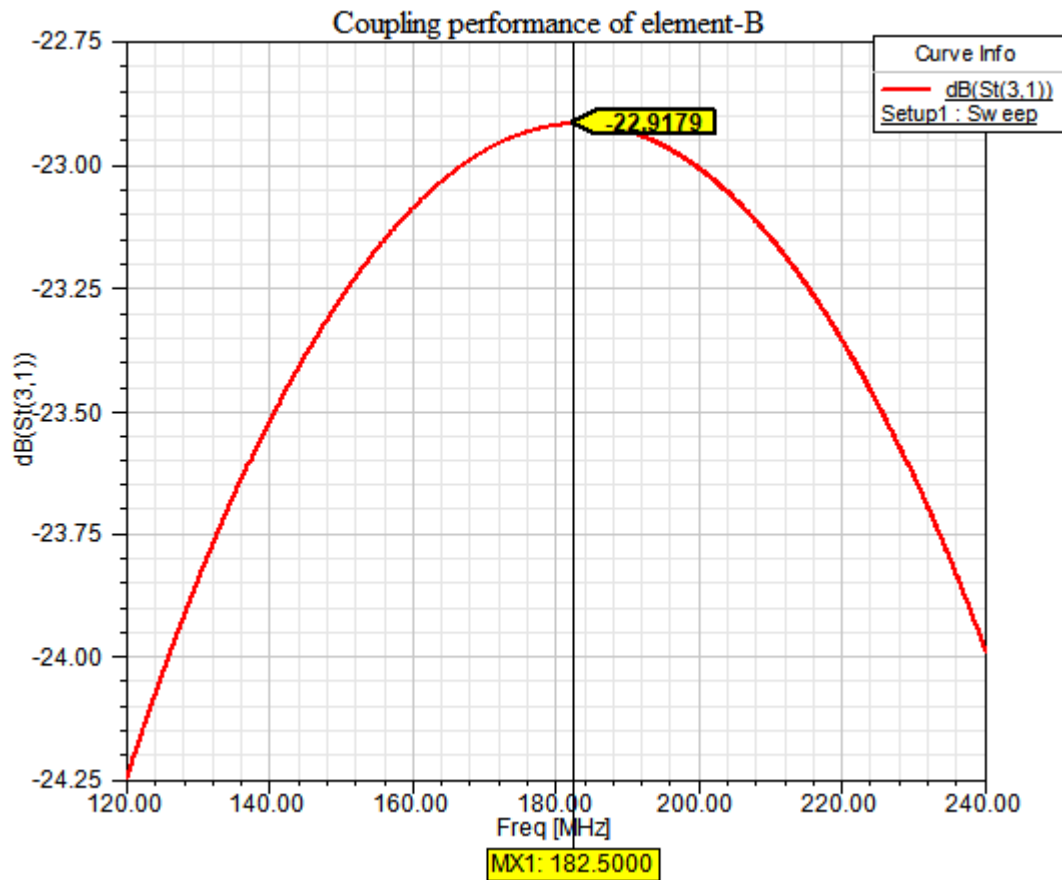


Fig. 6.3(b) Simulated result of Coupling for element-B using HFSS

The result shown in figure shows that at the centre frequency of 182.5MHz the coupling coefficient is nearly equal to the desired coupling of  $-22.896\text{dB}$ .

So, the result for element-A and element-B are verified at the centre frequency.

Next step is to connect a junction between these three elements namely B,A,B to achieve  $8.34 \pm 0.3\text{dB}$  coupling. For the given configuration, junction length of 5cm is provided in each element after joining the  $8.34 \pm 0.2\text{dB}$  coupler model is shown in Fig. 6.1 and the simulation result of  $8.34\text{dB}$  coupling is shown in Fig. 6.4.

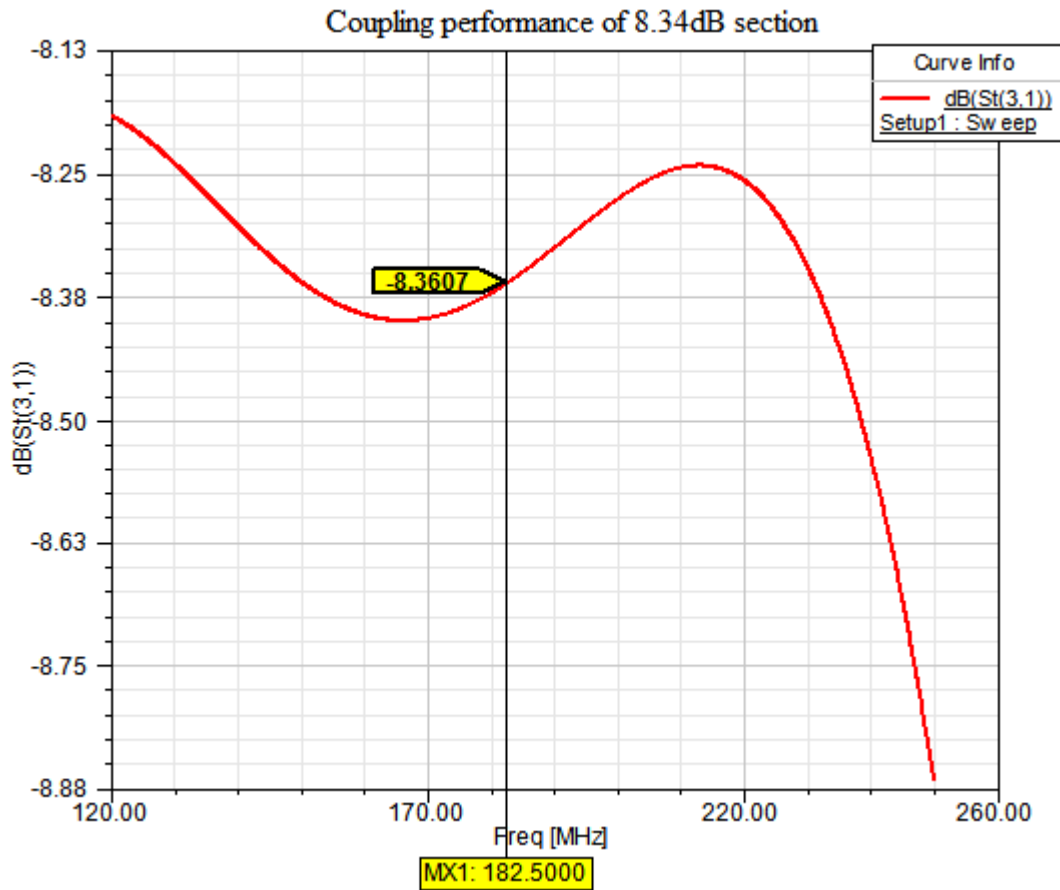


Fig. 6.4 Simulated result of 3-elements, 8.34dB coupled line section using HFSS.

Now, the next step is to connect two  $8.34 \pm 0.2dB$  sections in tandem to form desired coupling of  $3 \pm 0.4dB$ . Here, the design of ultra-wide band  $3 \pm 0.4dB$  tandem hybrid coupler of 50 Watt power handling capability and 130 to 240Mhz frequency range of VHF is covered and presented in Fig. 6.6.

The dimensions of connecting lines that are connected to join two section of 8.34dB section to make it 3dB are given below:

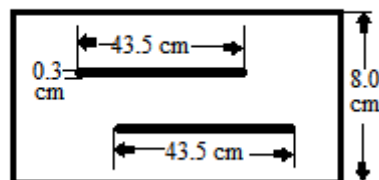


Fig.6.5 Dimensions of connecting line

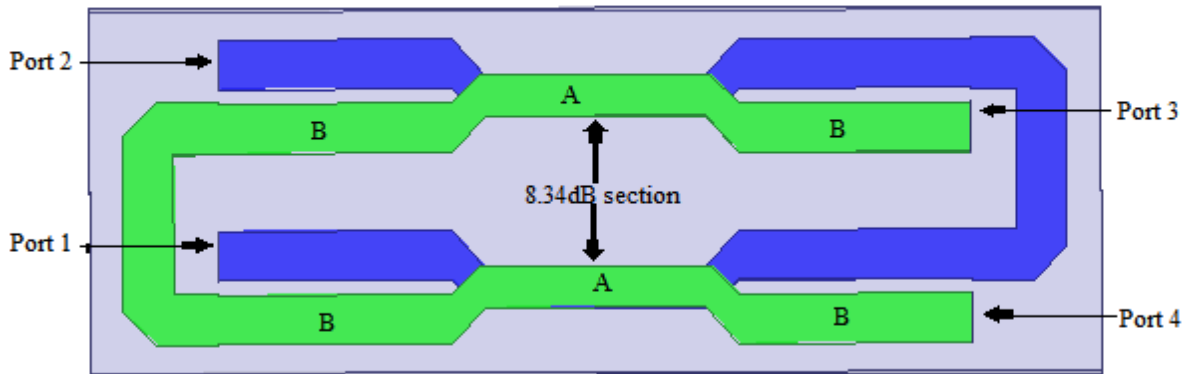


Fig. 6.6 Schematic 3dB tandem hybrid coupler of three elements.

The ultra-wide band 3dB hybrid coupler as shown in the Fig. 6.6 shows the two 8.34dB coupled lines connecting in tandem and the four ports through which we obtain our results. The results are obtained by calculating the S-parameters as shown below. The results show that the coupler works for an ultra-wide band range of frequency in the VHF band. Mainly from the application point of view, the hybrid coupler can be used in the experimental set-up of a Load resilient mock-up ICRH system of a tokamak with variable load. The use of a hybrid coupler ensures that no reflections return back to the generator when the reflections on the output are equal both in magnitude and in phase, which in this case are diverted to the dummy load. Fig. 6.7, 6.8, 6.9 and 6.10 show the return loss, output power, coupled power and the isolation.

### 6.3 Calculated S-Parameters for Three-element 3dB Tandem hybrid coupler.

#### 1. Return loss:-

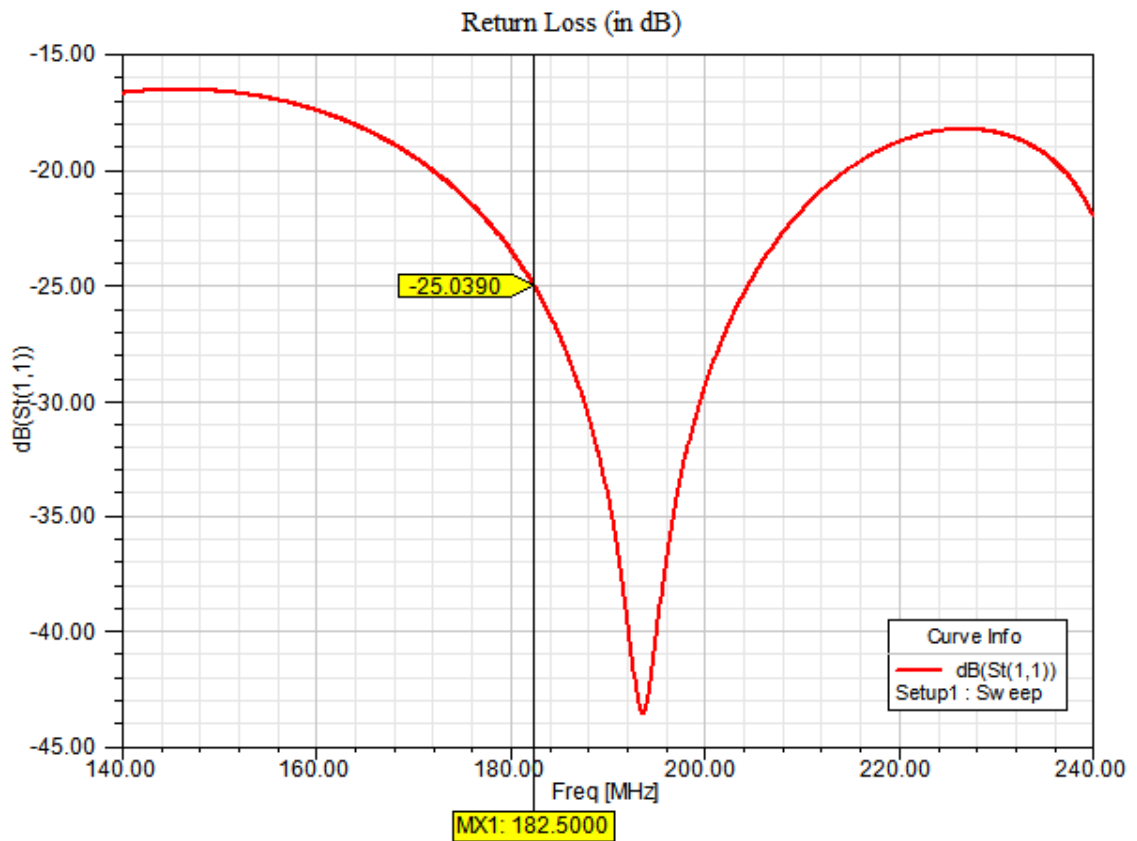


Fig. 6.7 Return Loss of 3dB tandem hybrid coupler for three element

The return loss represented as  $S_{11}$  determine how much power is reflected back to port1. At the center frequency of 182.5MHz, the return loss is calculated to be -25.04dB which is approximately .31 % of the input power.

## 2. Output power:-

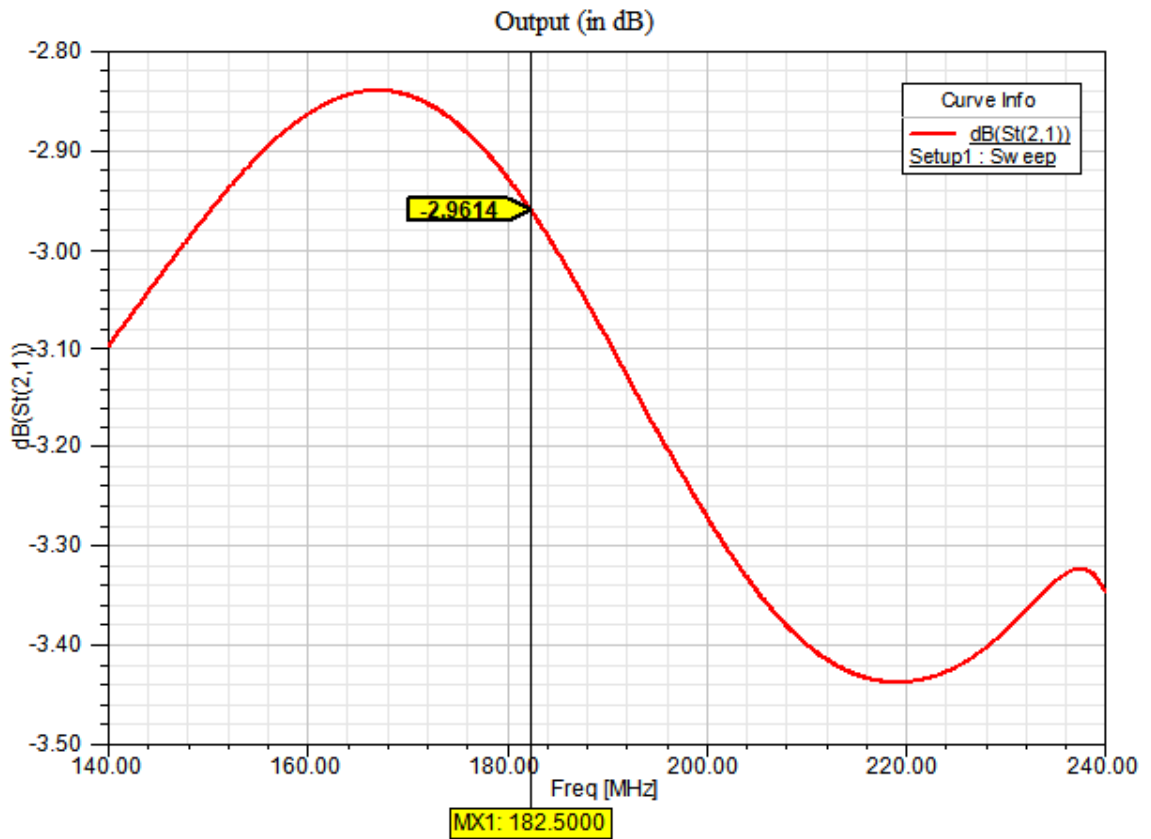


Fig. 6.8 Output of 3dB tandem hybrid coupler for three element

The output represented as  $S_{21}$  determine how much power is received at the output port when input power is given at port1. At the center frequency of 182.5MHz, the output is calculated to be -2.9614dB which is approximately 50 % of the input power.

### 3. Coupling power:-

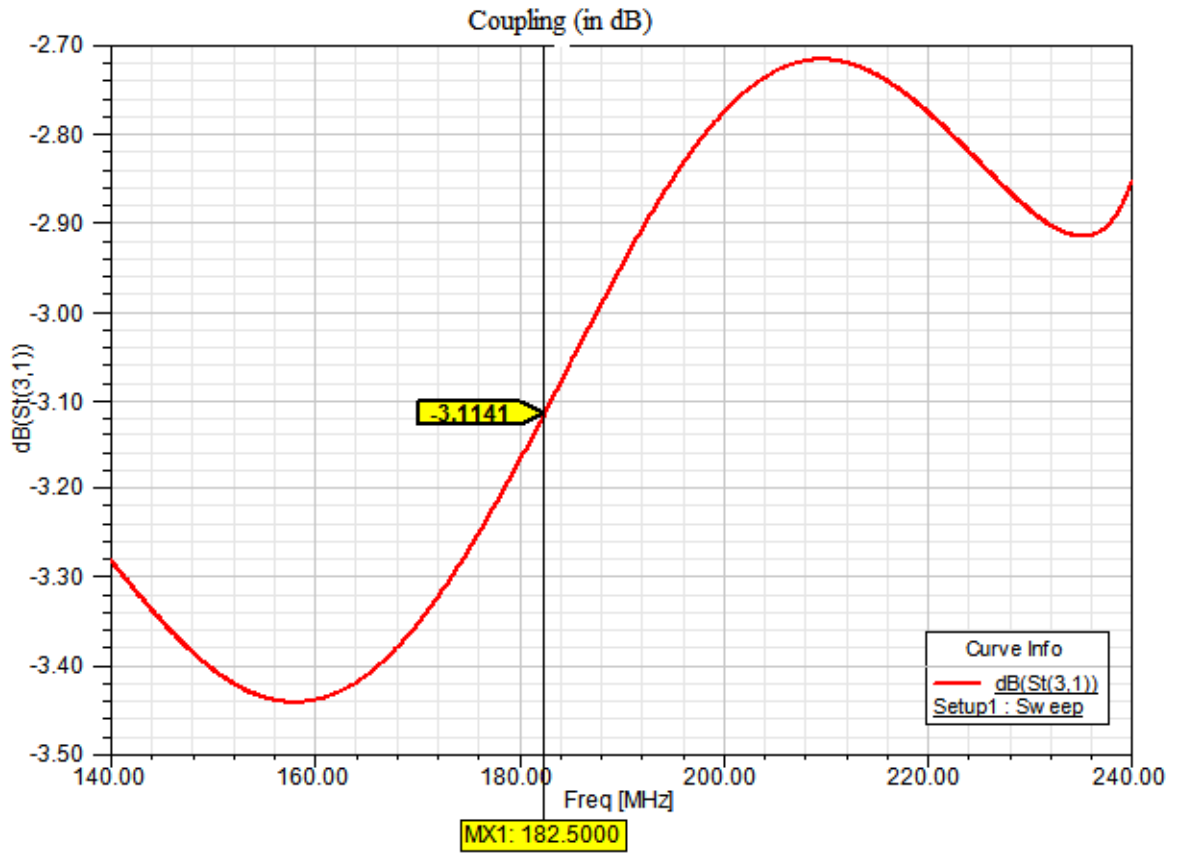


Fig. 6.9 Coupling of 3dB tandem hybrid coupler for three element

The coupling represented as  $S_{31}$  determine how much power is coupled to port 3 from input port. At the center frequency of 182.5MHz the coupling is calculated to be -3.1141dB which is approximately 50 % of the input power.

The figure shows that the coupling power can be obtained upto a significant band from 140MHz to 240MHz.

#### 4. Isolation:-

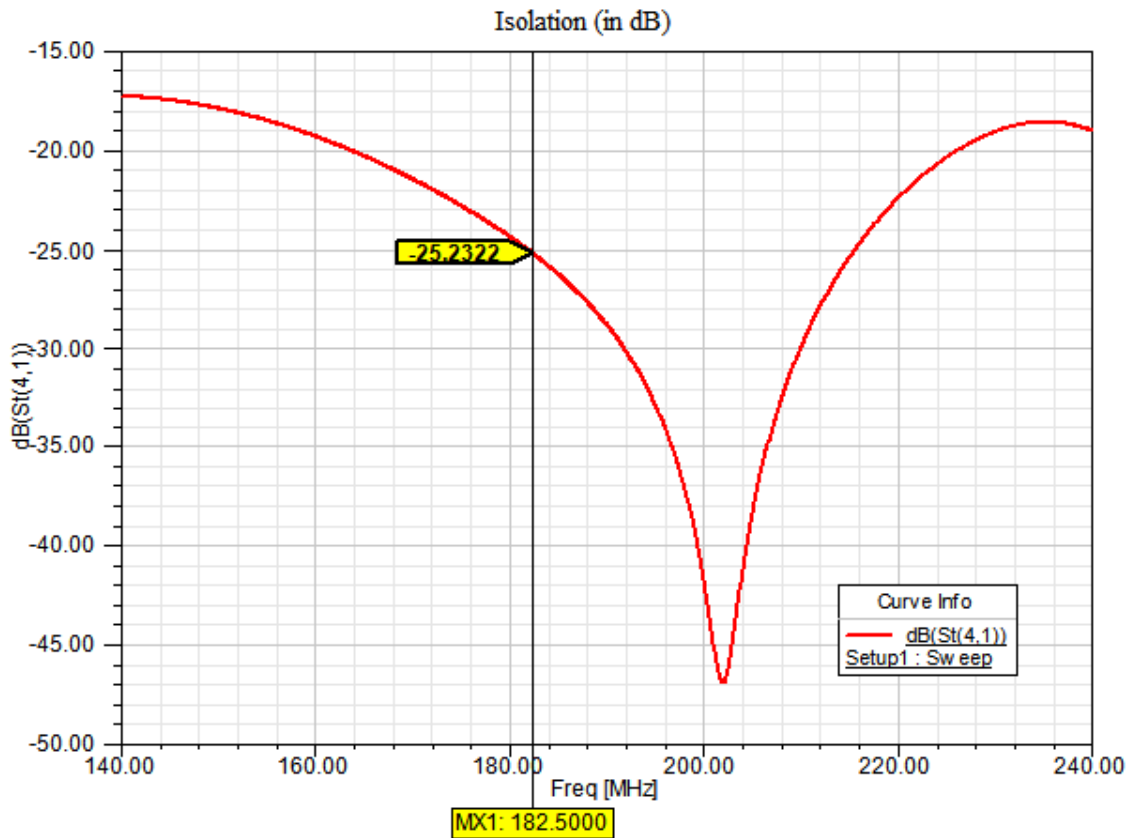


Fig. 6.10 Isolation of 3dB tandem hybrid coupler for three element

Isolation is defined as the difference in signal level between the input port and the isolated port when the other two ports are terminated by the matched load. At the center frequency of 182.5MHz, the isolation is calculated to be -25.23dB which is approximately .29 % of the input power.

### Concluding Remarks and Future Scope

---

#### 7.1 CONCLUSION

The dissertation presents the investigation on design and simulation of ultra-wide band 3dB tandem hybrid coupler for the load resilient mock-up fast RF matching network. The designed hybrid coupler works for the VHF range nearly 140MHz to 240MHz for the low power of about 50 Watt. The study has been done in various steps that are given as follows:

1. Initially, theory of single element and multi element coupled lines has been studied and analyzed using MATLAB software and coupling characteristics of both are presented in comparative manner.
2. Coupling of each of the cascaded elements is calculated using theory of equal ripple polynomial and it is found that coupling of middle element in multi-element coupled line coupler is very high which is difficult to achieve because of very thin slit in between coupled lines and thus the designing and fabrication of such coupler becomes impractical. The solution for this is the design of Tandem Coupler.
3. A narrow band single element 3dB hybrid coupler has been designed, simulated and presented.
4. Finally, a ultra-wide band 3dB tandem hybrid coupler with three elements is designed and simulated. The design has been simulated using HFSS and verified for the desired performance.

The developed ultra-wide band coupled lines can be used to achieve the wider bandwidth in RF components such as balanced amplifiers, balanced modulator, power measurements and antenna array networks. These components are utilized in the area of satellite communication, defense, broadcast, and aerospace.

## **7.2 FUTURE SCOPE**

The designing and simulation of single element hybrid tandem coupler has been carried out using HFSS and the future work will focus on its fabrication and testing which is useful for applications in narrow frequency band. For the broad band applications, multi-element hybrid tandem coupler has been designed and simulated and the focus will be laid on its fabrication in coming future. This hybrid coupler has to be used in the experimental set up of mock-up fast RF matching network.

## ***References***

- [1] Bernard M. Oliver, "Directional Electromagnetic Couplers," *Proc. IRE*, Vol.42, pp.1686-1692, Nov. 1954.
- [2] Crystal, E. G. and L. Young, "Theory and table of optimum symmetrical TEM-mode coupled transmission line directional coupler," *IEEE Trans. on Microwave Theory and Techniques*, Vol. 13, No. 5, 544-553, 1965.
- [3] W. L. Firestone, "Analysis of transmission line directional couplers," *Proceedings of the IRE*, 42(10):1529-1538, 1954.
- [4] David M. Pozar, Microwave Engineering, chapter 7, *John Wiley & Sons*, Inc. 4<sup>th</sup> ed., 2012, pp. 317-372.
- [5] Jim Stiles, "Coupled-Line Directional Couplers,"  
Internet:[http://www.ittc.ku.edu/~jstiles/723/handouts/section\\_7\\_6\\_Coupled\\_Line\\_Directional\\_Couplers\\_package.pdf](http://www.ittc.ku.edu/~jstiles/723/handouts/section_7_6_Coupled_Line_Directional_Couplers_package.pdf) , April.4, 2009[April.11,2015].
- [6] R. Levy, "General synthesis of asymmetric multi-element coupled-transmission-line directional couplers," *IRE Trans. on Microwave Theory and Techniques*, Vol. MTT-11, pp. 226 -237, Jul. 1963.
- [7] R. P. Yadav, S. Kumar and S.V. Kulkarni, "An analysis of junction discontinuity effects in multi-element coupled lines and its diminution at designing stage," *Progress In Electromagnetics Research B*, Vol. 56, pp. 25-49, 2013.
- [8] P. P. Toulous and A. C. Todd, "Synthesis of symmetrical TEM-mode directional couplers," *IEEE Trans. on Microwave Theory and Techniques*, Vol. MTT-13, pp. 536-544, Sep. 1965.
- [9] Valery A. Dolagashev and Sami G. Tantawi, "Effect of RF parameters on break down limits in high-vacuum x-band structures," *AIP Conference Proceedings*, pp. 151-165, 2003.

- [10] Sami G. Tantawi and Christopher D. Nantista, "Active and passive RF components for high power systems," *AIP Conference Proceedings*, pp. 83-100, 2002.
- [11] Peter A. Rizzi. *Microwave engineering*: John Wiley& Sons, 2009.
- [12] Robert M. Barnett, "Microwave printed circuits the early years: Microwave Theory and Techniques," *IEEE Transactions*, 32(9):983-990, 1984.
- [13] Seymour B. Cohn, "Parallel-coupled transmission-line-resonator filters: Microwave Theory and Techniques," *IRE Transactions on*, 6(2):223-231, 1958.
- [14] Harlan H. Howe, "Stripline circuit design," Artech House Dedham, M.A., 1974.
- [15] Robert E. Collin, "*Foundations for microwave engineering*," John Wiley & Sons, 2007.
- [16] K. C. Gupta, Tatuso Itoh and Arthur A. Oliner, "Microwave and RF education-past, present, and future: Microwave Theory and Techniques," *IEEE Transactions*, 50(3):1006-1014, 2002.
- [17] I. J. Bahl and K. C. Gupta, "Average power-handling capability of microstrip lines," *IEEE Journal in Microwaves, Optics and Acoustics*, 3(1):1-4. 1979.
- [18] Rana Pratap Yadav, S. Kumar, and S. Kulkarni, "Junction Discontinuity effect in Multi-element Coupled Lines and its Compensation," *IEEE Region 10 Symposium 2014*.
- [19] Yadav, R. P., S. Kumar, and S. V. Kulkarni, "Design and development of 3 dB patch compensated tandem hybrid coupler," *Rev. Sci. Instrum.*, Vol. 84, 014702, 2013.
- [20] Bharathi Bhat and Shiban K. Koul, "Stripline-like transmission lines for microwave integrated circuits," *New age International*, 1989.

- [21] R. Levy, "Transmission-line directional couplers for very broad-band operation," *Electrical Engineers, Proceedings of the Institution of Electrical Engineering*, Vol. 112(3), pp. 469-476, 1965.
- [22] E. M. T. Jones and J. T. Bolljahn, "Coupled-strip transmission line filters and directional couplers," *IRE Trans. on Microwave Theory and Techniques*, Vol. MTT-4, pp. 75-81; April, 1956.
- [23] J. Reed and G. J. Wheeler, "A method of analysis of symmetrical four port networks," *IRE Trans. on Microwave Theory and Techniques*, Vol. MTT-4, pp. 246-252, Oct. 1956.
- [24] H. J. Riblet, "General synthesis of quarter-wave impedance transformers," *IRE Trans. on Microwave Theory and Techniques*, Vol. MTT-5, pp. 36-43, Jan. 1957.
- [25] J. K. Shimizu and E. M. T. Jones, "Coupled transmission-line directional couplers," *IRE Trans. on Microwave Theory and Techniques*, Vol. MTT-6, pp. 403 -411, Oct. 1958.
- [26] Cohn, S. B., "Characteristic impedance of the broad-side coupled strip transmission line," *IRE Trans. On Microwave Theory Techniques*, Vol. 8, pp. 633-637, Nov. 1960. [27] L. Young, "The analytical equivalence of TEM-mode directional couplers and transmission line stepped-impedance filters," *Proc. IEE (London)*, Vol. 110, pp. 275-281, Feb. 1963.
- [28] R. Levy, "Tables for asymmetric multi-element coupled transmission line directional couplers," *IRE Trans. on Microwave Theory and Techniques*, Vol. MTT-12, pp. 275-279, May 1964.
- [29] H. Seidel and J. Rosen, "Multiplicity in cascade transmission line synthesis-part I," *IEEE Trans. on Microwave Theory and Techniques*, Vol. MTT-13, pp. 398-407, July 1965.

- [30] Person, C. L. Carre, E. Rius, J. P. Coupez, and S. Toutain, "Original techniques for designing wideband 3-D integrated Couplers," *IEEE MTT-S Int. Microw. Symp. Dig.*, pp. 119-122, 1998.
- [31] Dydyk, M., "General synthesis of symmetric multi-element coupled transmission line directional couplers," *IEEE Trans. Microwave. Theory Tech.*, Vol. 47, No. 6, 956-964, Jun. 1999.
- [32] Kats, B. M., V. P. Meschanov, and A. L. Khvalin, "Synthesis of superwide-band matching adapters in round coaxial lines," *IEEE Trans. on Microwave Theory and Techniques*, Vol. 49, No. 3, 575-579, Mar. 2001.
- [33] Bhat, B. and S. K. Koul, "Stripline-like a Transmission Lines for Microwave Integrated Circuit," *New Age International Publishers, India*, 2007, 138-139, 282-284.
- [34] Leo Young, "The analytical equivalence of TEM-mode directional couplers and transmission-line stepped-impedance filters," *Proceedings of the Institution of Electrical Engineers*, Vol. 110, pp. 275-281, IET, 1963.
- [35] Amendra Koul, Marina Y. Koledintseva, Scott Hinaga and James L. Drewniak, "Differential extrapolation method for separating dielectric and rough conductor losses in printed circuit boards," *Electromagnetic Compatibility, IEEE Transactions*, 54(2):421-433.2012.
- [36] Rana Pratap Yadav, Sunil Kumar and S. V. Kulkarni, "Design and development of ultra-wideband 3dB hybrid coupler for ion cyclotron resonance frequency heating in tokamak," *Review of Scientific Instruments*, 85(4):044706, 2014.
- [37] Rana Pratap Yadav, Sunil Kumar and S.V. Kulkarni, "Design of the 1.5MW, 30-96 MHz ultra-wideband 3dB high power hybrid coupler for Ion Cyclotron Resonance Frequency(ICRF) heating in fusion grade reactor," *Review of Scientific Instruments*, 87:014703(2016)

- [38] Seymour B. Cohn and Ralph Levy, "History of microwave passive components with particular attention to directional couplers," *Microwave Theory and Techniques, IEEE transactions*, 32(9):1046-1054, 1984.
- [39] N. S. Murthy Sarma, M. Chakrapani and P. Parvathi, "Design and Verification of Strip Line Directional Couplers for Various Applications in RF and Microwave Communication Systems," *International Journal of Computer Science and Information Technologies*, Vol. 2 (2):871-875, 2011
- [40] D. Bora, Sunil Kumar, Raj Singh, K. Sathyanarayana, S. V. Kulkarni, A. Mukherjee, B.K. Shukla, J.P. Singh, Y.S.S. Srinivas, P. Khilar, et al. Cyclotron resonance heating systems for SST-1. *Nuclear fusion*, 46(3):S72, 2006.
- [41] M. Mayoral, I. Monakhov, T. Walden, V. Bobkov, T. Blackman, M. Graham, J. Mailloux, J. Noterdaeme, M. Nightingale, and J. Ongena, "Hybrid couplers on the jet icrf system: Commissioning and first results on elms," *AIP Conference Proceedings*, Vol. 933, pp. 143, 2007.
- [42] Chul-Soo Kim, Jong-Sik Lim, Dong-Joo Kim, and Dal Ahn, "A design of single and multi-section microstrip directional coupler with the high directivity," *Microwave Symposium Digest, 2004 IEEE MTT-S International*, Vol. 3, pp. 1895-1898, 2004.
- [43] Sarmad Al-Taei, Phil Lane and George Passiopoulos, "Design of high directivity directional couplers in multilayer ceramic technologies," *Microwave Symposium Digest, 2001 IEEE MTT-S International*, Vol. 1, pp. 51-54, 2001.

# THESIS

---

## ORIGINALITY REPORT

---

<b>12%</b>	<b>4%</b>	<b>10%</b>	<b>2%</b>
SIMILARITY INDEX	INTERNET SOURCES	PUBLICATIONS	STUDENT PAPERS

---

## PRIMARY SOURCES

---

- 1** Yadav, Rana Pratap, Sunil Kumar, and S. V. Kulkarni. "Junction discontinuity effect in multi-element coupled lines and its compensation", 2014 IEEE REGION 10 SYMPOSIUM, 2014. **2%**  
Publication
- 2** Inder J. Bahl. "Average power handling capability of multilayer microstrip lines", International Journal of RF and Microwave Computer-Aided Engineering, 11/2001 **1%**  
Publication
- 3** "Abstracts of IRE Transactions", Proceedings of the IRE, 1959 **1%**  
Publication
- 4** Submitted to Universiti Tenaga Nasional **1%**  
Student Paper
- 5** Gupta, K.C. Itoh, Tatsuo Oliner, Arthur . "Microwave and RF education--past, present, and future.(Abstract)", IEEE Transactions on Microwave Theory an, March 2002 Issue **1%**  
Publication
- 6** Wu. "Design of Microwave Circuits", Software